Engineering Fracture Mechanics 187 (2018) 381–403

Contents lists available at ScienceDirect

Engineering Fracture Mechanics

journal homepage: www.elsevier.com/locate/engfracmech

Review

A local approach to cleavage fracture modeling: An overview of progress and challenges for engineering applications

Claudio Ruggieri [a,*], Robert H. Dodds Jr. [b]

[a] Dept. of Naval Architecture and Ocean Engineering, University of São Paulo, São Paulo, Brazil
[b] Dept. of Civil and Environmental Engineering, University of Illinois at Urbana-Champaign, IL, USA

ARTICLE INFO

Article history:
Received 3 November 2017
Received in revised form 13 December 2017
Accepted 13 December 2017
Available online 14 December 2017

Keywords:
Cleavage fracture
Local approach
Weibull stress
Plastic strain
Constraint effects

ABSTRACT

This paper provides an overview of recent progress in probabilistic modeling of cleavage fracture phrased in terms of a local approach to fracture (LAF) and the Weibull stress concept. Emphasis is placed on the incorporation of plastic strain effects into the probabilistic framework by approaching the strong influence of constraint variations on (macroscopic) cleavage fracture toughness in terms of the number of eligible Griffith-like microcracks which effectively control unstable crack propagation by cleavage. Some recent results based on a modified Weibull stress model to predict specimen geometry effects on J_c-values for pressure vessel grade steels are summarized in connection with an engineering procedure to calibrate the Weibull stress parameters. These results are compared against corresponding fracture toughness predictions derived from application of the standard Beremin model. Finally, the robustness of LAF methodologies, including specifically the Weibull stress approach, is critically examined along with a discussion of key issues and challenges related to engineering applications in fracture assessments of structural components.

Contents

* Corresponding author.
E-mail address: claudio.ruggieri@usp.br (C. Ruggieri).

https://doi.org/10.1016/j.engfracmech.2017.12.021
0013-7944/

1. Introduction

The increased demand for more accurate structural integrity and fitness-for-service (FFS) analysis of a wide class of engineering structures, including nuclear reactor pressure vessels, piping systems and storage tanks, has stimulated renewed interest in advancing current safety assessment procedures of critical structural components, including life-extension programs and repair decisions of aging structures. Simplified fracture mechanics based approaches for quantitative analysis of material degradation, as of interest in assessments of crack-like flaws formed during in-service operation, focus primarily on the potential for catastrophic failure due to low toughness behavior. Specifically for ferritic materials at temperatures in the ductile-to-brittle transition (DBT) region, such as carbon and low-alloy steels typically used in many structural applications, unstable fracture by transgranular cleavage still represents one the most serious failure modes as local crack-tip instability may trigger catastrophic structural failure at low applied stresses with little plastic deformation. These methods, also referred to as engineering critical assessment (ECA) procedures, rely on direct application of macroscopic measurements of cleavage fracture toughness (such as the J-integral at cleavage instability, J_c, or the critical Crack Tip Opening Displacement, CTOD or δ_c) derived from conventional fracture specimens tested under high constraint conditions, similar to those of small-scale yielding (SSY), to define conservative flaw acceptance criteria. While conventional ECA methodologies clearly simplify integrity assessments of in-service structural components, they have limited ability to predict the potential strong influence of constraint on fracture behavior and, perhaps more importantly, do not address the strong sensitivity of cleavage fracture to material characteristics at the microlevel.

The early recognition of these limitations prompted a surge of interest in analyzing, predicting and unifying toughness measures across different crack configurations and loading modes based on a micromechanics interpretation of the cleavage fracture process. Here, attention has been primarily focused on probabilistic models incorporating weakest link statistics, most often referred to as local approaches to fracture (LAF) [1–3], to describe material failure caused by transgranular cleavage for a wide range of loading conditions and crack geometries. In the context of probabilistic fracture mechanics, the methodology yields a limiting distribution that describes the coupling of the (local) fracture stress with remote loading (as measured by J or CTOD) in terms of a fracture parameter characterizing macroscopic fracture behavior for a wide range of loading conditions and crack configurations. Among these earlier research efforts, the seminal work of the French group Beremin [1] provided the impetus for development of a framework establishing a relationship between the microregime of fracture and macroscopic crack driving forces (such as the J-integral) by introducing the Weibull stress (σ_w) as a probabilistic fracture parameter directly connected to the statistics of microcracks (weakest link philosophy). A key feature of this methodology is that σ_w incorporates both the effects of stressed volume (the fracture process zone) and the potentially strong changes in the character of the near-tip stress fields due to constraint loss which thus provides the necessary framework to correlate fracture toughness for varying crack configurations under different loading (and possibly temperature and strain rate) conditions. Previous research efforts to develop a transferability model to elastic-plastic fracture toughness values rely on the notion of the Weibull stress as a crack-tip driving force [4–7] by adopting the simple axiom that unstable crack propagation (cleavage) occurs at a critical value of the Weibull stress, $\sigma_{w,c}$.

However, a fundamental objection to the probabilistic framework from which the Weibull stress concept is derived is that it relies on the assumption that Griffith-like microcracks (which effectively act as precursors of transgranular cleavage in structural steels [8]) form immediately upon the onset of yielding thereby implying that the associated statistical distribution of microcrack size remains unchanged with increased loading and deformation. Experimental evidence for the coupling between microcrack size distribution and plastic deformation has been given in the early works of McMahon and Cohen [9], Kaechele and Tetelman [10], Brindley [11], Lindley et al. [12] and Gurland [13]. These studies observed the strong effects of plastic strain on cleavage microcracking in ferritic steels at varying temperatures which can lead to a marked influence on the density of Griffith-like microcracks directly connected to the material fracture behavior at the microscale. Here, the number of microcracks formed from fractured carbide particles within a small, near-tip material volume increases with increased plastic strain. Since any cleavage fracture model incorporating statistics of microcracks (weakest link philosophy), such as the σ_w-based methodology, involves a local Griffith instability of the largest, most favorably oriented microcrack, it becomes clear that increased plastic strains correlate directly with increased likelihood of cleavage failure. To some extent, these difficulties can be overcome by incorporating explicitly the influence of plastic strain into the micromechanism of cleavage failure entering directly into the probabilistic description of fracture. But how the controlling microstructural features - microcrack size distribution and plastic strain level - are interconnected and their relative contributions to the macroscopic fracture behavior (and associated failure probability) remain open issues.

This paper provides an overview of recent progress in probabilistic modeling of cleavage fracture phrased in terms of a local approach to fracture (LAF) and the Weibull stress concept. Emphasis is placed on the incorporation of plastic strain effects into the probabilistic framework by approaching the strong influence of constraint variations on (macroscopic) cleavage fracture toughness in terms of the number of eligible Griffith-like microcracks which effectively control unstable crack propagation by cleavage. Some recent results based on a modified Weibull stress model to predict specimen geometry effects on J_c-values for pressure vessel grade steels are summarized in connection with an engineering procedure to calibrate the Weibull stress parameters. These results are compared against corresponding fracture toughness predictions derived from application of the standard Beremin model. Finally, the robustness of LAF methodologies, including specifically the Weibull stress approach, is critically examined along with a discussion of key issues and challenges related to engineering applications in fracture assessments of structural components.

2. The Weibull stress approach incorporating plastic strain effects

The development of probabilistic approaches for cleavage fracture has seen continuous progress since the pioneering work of Weibull [14,15] who brought the weakest link interpretation of fracture (in connection with a random distribution of Griffith-like microcracks dispersed in the material) to bear on the problem of predicting size effects on fracture in terms of a convenient probability distribution for the fracture strength of brittle materials. Subsequently, Epstein [16] and later Freudenthal [17] advanced the viewpoint of the weakest link concept to introduce a mathematical description for the fracture strength of materials in terms of the statistical theory of extreme values [18,19]. Building upon Weibull's work and using purely statistical arguments, they showed that the distribution of the fracture strength for a stressed solid associated with the weakest link concept depends on the assumed functional form for the fracture resistance of Griffith-like microcracks randomly distributed in a given volume of material. Such a viewpoint is often referred to as the elemental strength approach [20] and derives from the assumption that a stressed body contains a random distribution of Griffith-like microflaws or microcracks which can be characterized by their fracture stress at which the Griffith cleavage condition is met (termed the "microflaw strength" by Epstein [16]). Several probabilistic models have been proposed based on the elemental strength approach to develop limiting distributions for the fracture stress and to predict size effects in fracture, including the works of McClintock and Argon [21], Batdorf and Crose [22], Evans [23], McClintock and Zaverl [24], Matsuo [25], Lin et al. [26], Godse and Gurland [27], among others.

Another line of development which shares much in common with the elemental strength approach is based on the statistics of microcracks contained in the stressed material volume. A number of research efforts in this area have explicitly adopted convenient functional forms describing the microcrack size (and possibly orientation) to define a limiting distribution for the cleavage fracture stress. The early work of Freudenthal [17] and later Evans and Langdon [20] devised the connection between the statistical distribution of microcrack size and the distribution function of the local fracture stress based on theoretical arguments derived from the extreme value theory [19]. Subsequent researchers adopting this class of approach include Beremin [1], Wallin and co-workers [28,29], Mudry [2], Pineau [30], Minami et al. [31], Ruggieri and Dodds [4], Gao et al. [32], Petti and Dodds [33] and Ruggieri [34]. Work of the French Beremin group [1] attains particular relevance as it has served as the basis for generalizing the concept of micromechanics modeling for cleavage fracture which in turn has enabled the development of approaches highly effective in unifying toughness measures across different crack configurations and loading modes. Further advancements in micromechanics modeling of cleavage fracture incorporating a more realistic physical mechanism of cleavage microcrack nucleation and propagation have also been made with the Prometey model [35–37] and also in the representative works of Faleskog et al. [38,39], Hohe et al. [40–42] and James et al. [43]. An overview of these local approach developments is given by Pineau [3].

This section reviews the fundamental concepts of the analytical framework that have a direct bearing on the probabilistic modeling of cleavage fracture from which the Weibull stress approach is derived. Only salient features of the probabilistic framework are discussed here. We begin by providing an overview of the Beremin model and associated limiting distribution for the cleavage fracture stress of a cracked body which have been extensively used in multiscale predictions of fracture behavior in structural components with diverse range of crack-tip constraint. We then turn attention to a modified form of the Weibull stress incorporating the effects of plastic strain on cleavage fracture coupled with statistics of microcracks which are not fully accounted in conventional analyses using the standard Beremin model. Other developments in local approaches to cleavage fracture modeling are also briefly mentioned since there has been considerable interplay in recent years between different treatments of plastic strain effects and more specific statistical models for cleavage fracture. Readers are referred to the works of Ruggieri and Dodds [6,7] and references therein for a more complete discussion of the Weibull stress methodology, and the review articles by Pineau [3], Pineau and Tanguy [44], Pineau et al. [45] for other microstructural details.

2.1. The Weibull stress as a probabilistic crack driving force

A substantial number of studies and experimental observations have provided detailed descriptions of the cleavage fracture process [46–48]. A number of works, including that of Low [49], Owen et al. [50], McMahon and Cohen [9] and Smith [48], revealed that the formation of Griffith-like microcracks [51] after the onset of yielding and localized plasticity, primarily

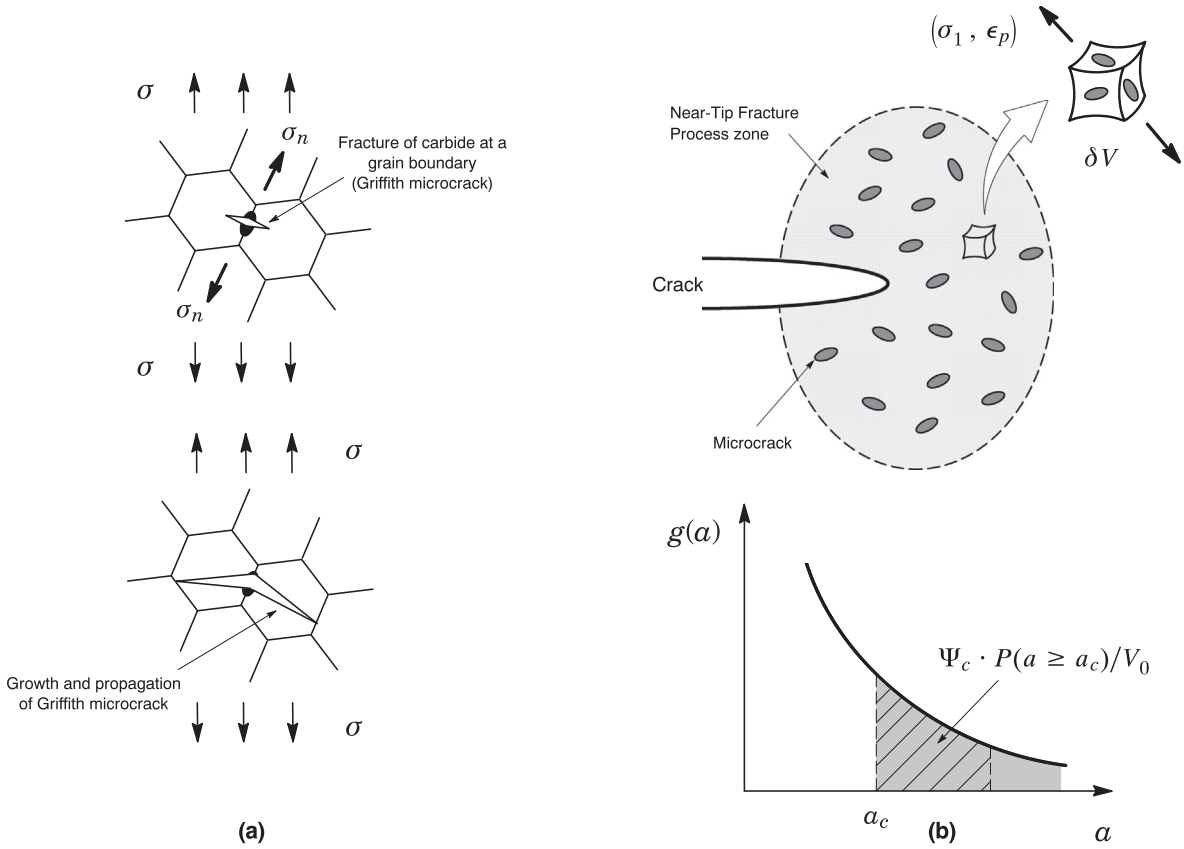

Fig. 1. (a) Near-tip fracture process zone ahead a macroscopic crack containing randomly distributed flaws. (b) Schematic of power-law type microcrack size distribution.

by the cracking of hard, particle-like brittle phases such as carbides along grain boundaries, governs cleavage fracture of ferritic steels. This process occurs over one or two grains of the polycrystalline aggregate; once a microcrack has formed in a grain and spread through the nearby ferrite grain boundaries, it likely propagates by a cleavage mechanism with no significant increase in the applied stress unless the microcrack is arrested at a high-angle grain boundary [8]. The connection between fracture resistance and microstructure can then be made by rationalizing the interrelation between microcrack nucleation and unstable propagation as illustrated in Fig. 1(a): (*i*) fracture of a carbide particle assisted by plastic deformation of the surrounding matrix nucleates a Griffith-like microcrack; (*ii*) the nucleated microcrack advances rapidly into the interior of the ferrite grain until it reaches a grain boundary and (*iii*) fracture occurs when the microcrack is not arrested at a grain boundary barrier and thus propagates unstably. In terms of the Griffith cleavage criterion [51], the last condition means that the Griffith fracture energy to propagate the microcrack is larger than the specific surface energy of the grain boundary [8].

To arrive at a tractable form of the cleavage fracture process outlined above, we consider an arbitrarily stressed body where a macroscopic crack lies in a material containing randomly distributed flaws as illustrated in Fig. 1(b). The fracture process zone ahead of the (macroscopic) crack tip is defined as the highly stressed region where the local operative mechanism for cleavage takes place; this region contains the potential sites for cleavage cracking. For the purpose of developing a probabilistic model for cleavage fracture, consider the fracture process zone ahead of the crack tip divided in a large number of unit volumes statistically independent; each unit volume contains a substantial number of statistically independent, Griffith-like microflaws uniformly distributed.

The statistical nature of this fracture process thus underlies a simplified treatment for unstable crack propagation of the configuration represented in Fig. 1(b). Based upon probability theory and invoking the well-known Poisson postulates (see, e.g., Feller [52]), the elemental failure probability, δP, is related to the distribution of the largest flaw in a reference volume of the material, which can be expressed as

$$\delta P = \delta V \int_{a_c}^{\infty} g(a) da \tag{1}$$

where $g(a)da$ defines the probability of finding a microcracks having size between a and $a + da$ in the unit volume [20,26]. Two fundamental assumptions based upon probability theory and the well-known Poisson postulates (see, *e.g.*, Feller [52]) underlie development of the above expression: (1) failures occurring in nonoverlapping volumes are statistically independent events, and (2) the probability of failure for small δV is proportional to its volume, *i.e.*, $\delta P = \mu \delta V$, where the proportionality constant μ is the average number of flaws with size $a \geqslant a_c$ per unit volume which are eligible to propagate unstably. Here, extreme value conditions associated with the standard probabilistic framework for cleavage fracture require a Cauchy-type distribution of microflaw size in the form $g(a) = (1/V_0)(\zeta_0/a)^{\varsigma}$, where ζ_0 and ζ are parameters of the distribution and V_0 denotes a reference volume [17,23], most often set as unit for convenience.

Now, the implicit distribution of fracture stress can be made explicit by introducing the dependence between the critical microcrack size, a_c, and stress in the form $a_c = K_{Ic}^2/(Y\sigma_{eq}^2)$, where K_{Ic} is the (local) fracture toughness of the material ahead of microflaw, Y represents a geometry factor and σ_{eq} denotes an equivalent (effective) tensile (opening) stress acting on the microcrack plane. Thus, if the maximum principal stress criterion is adopted, such as $\sigma_{eq} = \sigma_1$, the probability distribution, P_f, for the cracked body becomes [9, 22–25]

$$P_f(\sigma_1) = 1 - \exp\left[-\frac{1}{V_0}\int_{\Omega}\left(\frac{\sigma_1}{\sigma_u}\right)^m dV\right] \tag{2}$$

which can be rewritten as

$$P_f(\sigma_w) = 1 - \exp\left[-\left(\frac{\sigma_w}{\sigma_u}\right)^m\right] \tag{3}$$

such that the Weibull stress, σ_w, a term coined by Beremin [1], is defined by

$$\sigma_w = \left[\frac{1}{V_0}\int_{\Omega}\sigma_1^m d\Omega\right]^{1/m} \tag{4}$$

where Ω is the volume of the near-tip fracture process zone most often defined as the loci where $\sigma_1 \geqslant \psi\sigma_{ys}$, with σ_{ys} denoting the material's yield stress and $\psi \approx 2$, $\sigma_1 = \sigma_{eq}$ is the maximum principal stress acting on material points inside the FPZ. The above expression (3) defines a two-parameter Weibull distribution [53] for the random variable σ_w, in which parameters m and σ_u denote the Weibull modulus and the scale parameter of the Weibull distribution. In particular, m defines the shape of the probability density function describing the microcrack size, a, which is of the form $g(a) \propto a^{-\varsigma}$ with $m = 2\zeta - 2$. Moreover, since the reference volume, V_0, only scales $g(a)$ but does not change the distribution shape, it has no effect on m and is conveniently assigned a unit value in the computations.

In a related work, Lei [54,55] revisited the Beremin model and raised several concerns regarding key fundamental concepts related to the Weibull stress approach. Following statistical arguments essentially similar as those outlined above, Lei motivated his interpretation of a potential drawback in the Beremin model by introducing a threshold fracture stress, σ_{th} , into the probabilistic formulation, such that σ_1 should be replaced by $\sigma_1 - \sigma_{th}$ in previous Eq. (2), and then comparing his modified failure probability distribution with the corresponding distribution derived from the Beremin model. While Lei's approach addresses the open (and often neglected) question of the potential effects of a threshold fracture stress on fracture predictions based on the present methodology, his work overlooked a fundamental concept associated with the introduction of a threshold parameter into the above Eq. (2) in which parameter σ_u must change when σ_1 is replaced by $\sigma_1 - \sigma_{th}$ so that the nature of the cumulative probability distribution defined by that expression is still preserved. For example, Fig. 2 in [54] provides an untenable result for a simple case of uniaxial tension as the same value of 2000 MPa for the scale parameter (termed as σ_0 in Lei's work) of both Weibull distributions was adopted in his analysis – other analyzed cases in [54] also adopted a fixed value for the scale parameter so direct one-to-one comparisons are not possible. Similar arguments also hold true for the discussions and comparative analysis provided in [55]. Here, his conclusions also remain elusive as they follow from incorrect interpretation of Eq. (1) and subsequent expressions. In particular, Lei [55] imposes that $p = \int_{a_c}^{\infty} g(a)da$ associated with Eq. (23) of his paper must span the full range $0 \leqslant p \leq 1$, which is not necessarily correct. This is exactly what Fig. 1(b) clearly shows as $p = \int_{a_c}^{\infty} g(a)da$ simply defines the probability of finding a microcrack having size equal or larger than a_c and, thus, there is no conflict with any axiom of probability as stated in [55] since the survival probability would be $1 - \int_{a_c}^{\infty} g(a)da$. Indeed, when the critical microcrack size becomes very small, *i.e.*, as $a_c \to 0$ then $p \to 1$ implying that the material can be viewed as extremely brittle within the present context.

2.2. Inclusion of plastic strain effects: a modified Weibull stress

Recent treatments of the Beremin model have focused primarily on the effects of plastic strain on cleavage microcracking in ferritic steels and, thus, on cleavage failure probability. As already noted, a potential drawback with this model lies in the non-recognition of the prominent role played by the plastic strain at the microlevel on cleavage fracture thereby ignoring to a large extent the influence of the imposed near-tip stress *and* strain history on the cleavage failure probability. The Beremin approach assumes that all eligible microcracks nucleate immediately upon yielding so that their distribution does not

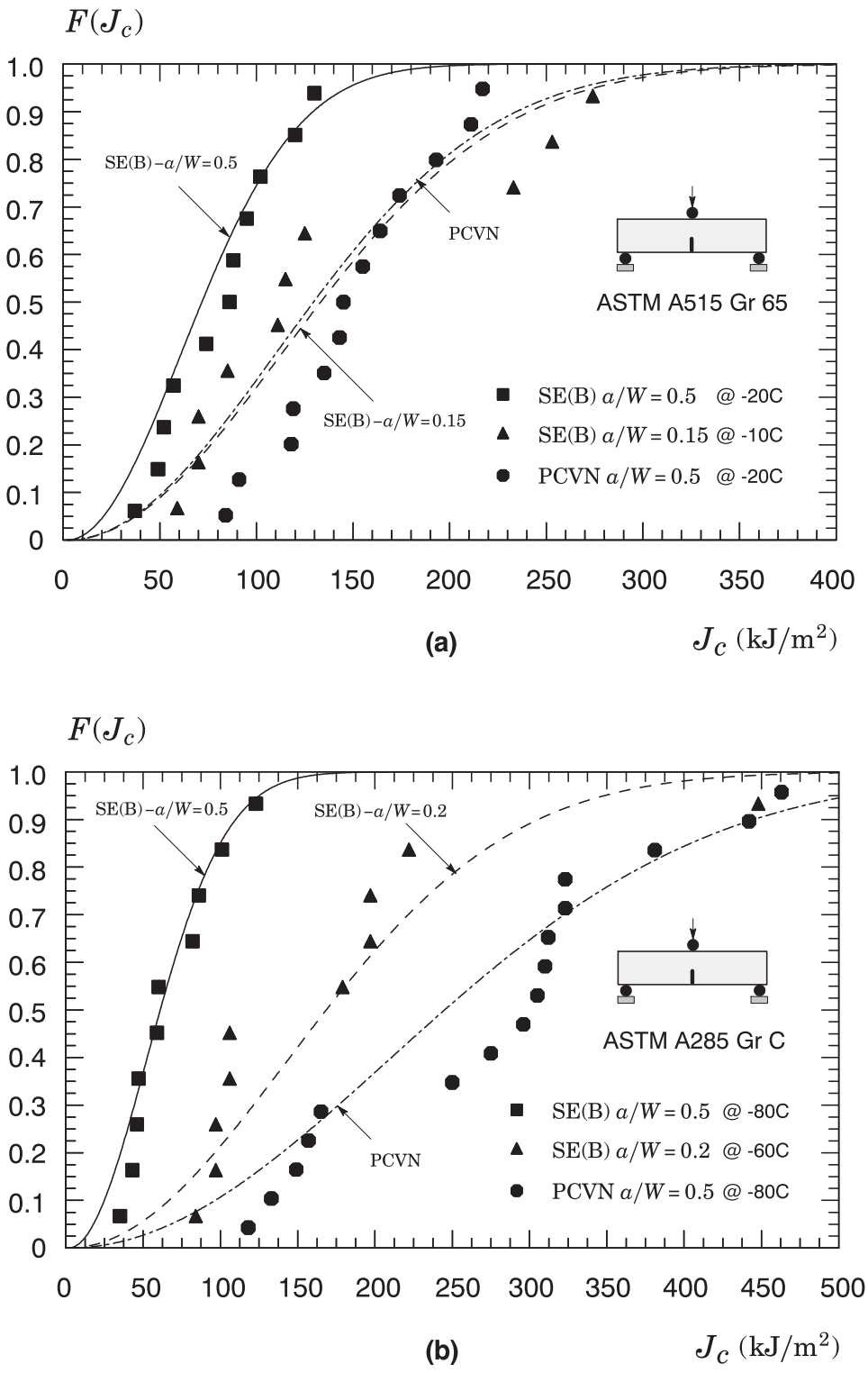

Fig. 2. Cumulative Weibull distribution of experimentally measured J_c-values for all tested specimen geometries and materials: (a) A515 Gr 65 steel reported by Ruggieri et al. [7]; (b) A285 Gr C steel tested by Savioli and Ruggieri [61].

change throughout the entire load history, which does not seem consistent with the history of experimental evidence linking the increase of microcrack density with increased plastic strain [9–13]. While the Beremin model clearly represented a significant advance in developing a simplified and yet highly effective methodology for fracture assessments of cracked

structural components subjected to various conditions, it also remains apparent that further enlargement on the probabilistic framework from which the approach derives is needed to include plastic strain effects.

Methodologies to incorporate effects of plastic strain into the Weibull stress model have evolved along essentially two lines of development: approaches that define the cleavage failure probability in dissociated form based on the notion that the microstructural process of cleavage fracture is driven by both the local stresses and plastic strains, and approaches that evaluate the cleavage failure probability based on the statistical distribution of Griffith-like microcracks. Research falling into the first category, including the works of Xia and Shih [56], Bordet et al. [57,58] and Margolin et al. [36], generally views the statistical problem of cleavage fracture by considering microcrack nucleation and propagation as two statistically independent events so that the cleavage fracture probability, P_c, is expressed by the standard product $P_n \times P_p$, where P_n is the probability of microcrack nucleation and P_p is the probability of microcrack propagation – note here that, when $P_n = 1$ and a convenient functional form describing the microcrack size is adopted to evaluate P_p, then the cleavage fracture probability, P_c, should yield a similar expression as given by the Beremin model. The latter category of approaches includes the previous study of Lin et al. [26], James et al. [59] and the more recent work of Ruggieri and Dodds (R&D) [6,7]. More specifically, R&D focused on incorporating the effects of plastic strain directly into the Beremin model and adopted the viewpoint that only Griffith-like microcracks formed from the cracking of brittle particles, such as carbide particles at grain boundaries in ferritic steels, in the course of plastic deformation contribute to cleavage fracture and, further, the fraction of fractured particles increases with increased matrix plastic strain. The R&D framework shares the essential features of the weakest link concept but addresses the strong effects of constraint variations on (macroscopic) cleavage fracture toughness by including the influence of plastic strain on the number of eligible Griffith-like microcracks which effectively control unstable crack propagation by cleavage.

R&D further approached the probabilistic coupling of cleavage fracture and plastic strain by considering that only a fraction, Ψ_c, of the total number of brittle particles in the FPZ nucleates the microcracks which are eligible to propagate unstably and that Ψ_c is a function of plastic strain but plausibly independent of microcrack size as pictured in Fig. 1(b). This approximation simplifies the treatment of the elemental failure probability associated with δV to arrive at a closed form for the failure probability of the stressed cracked body similar to previous Eq. (1) and expressed as

$$\delta P_f = \delta V \cdot \Psi_c(\epsilon_p) \cdot \int_{a_c}^{\infty} g(a) da \tag{5}$$

Following standard procedures based on the weakest link approach (see R&D [6]), a limiting distribution for the cleavage fracture stress can expressed as a two-parameter Weibull function [53] in the form

$$P_f(\sigma_1,\ \epsilon_p) = 1 - \exp\left[-\frac{1}{V_0}\int_{\Omega} \Psi_c(\epsilon_p) \cdot \left(\frac{\sigma_1}{\sigma_u}\right)^m d\Omega\right] \tag{6}$$

where Ω is the volume of the near-tip fracture process zone already defined and parameters m and σ_u appearing in Eq. (6) denote again the Weibull modulus and the scale parameter of the Weibull distribution for the fracture stress incorporating plastic strain effects. The above integral evaluated over Ω contains two contributions: one is from the principal stress criterion for cleavage fracture characterized in terms of σ_1 and the other is due the effective plastic strain, ϵ_p, which defines the number of eligible Griffith-like microcracks nucleated from the brittle particles effectively controlling cleavage fracture. Similar to the Beremin model [1], a simple manipulation of Eq. (6) then motivates the notion of a modified Weibull stress, $\tilde{\sigma}_w$, defined by

$$\tilde{\sigma}_w = \left[\frac{1}{V_0}\int_{\Omega} \Psi_c(\epsilon_p) \cdot \sigma_1^m d\Omega\right]^{1/m}. \tag{7}$$

where it is noted that setting $\Psi_c = 1$ recovers the standard Beremin model.

A number of options could be adopted in the above Eq. (7) for choosing a convenient form to define the fraction of fractured particles, Ψ_c. While a method of directly measuring Ψ_c would be most desirable, it is not very feasible nor practical in the context of routine applications of the methodology. Thus, it must be expected that, in general, the function Ψ_c chosen would reasonably describe the actual metallurgical and micromechanical features of the tested material in connection with the available experimental data. R&D [6] employ various forms of Ψ_c on fracture assessments and toughness predictions for low constraint crack configurations based on the present framework without, however, drawing definitive conclusions on the best choice. Section 3 provides further discussion of these points and gives a route to arrive at a simpler form for the failure probability of cleavage fracture including effects of plastic strain.

3. Applications in fracture testing

The following sections provide representative applications of the probabilistic framework for cleavage fracture assessments incorporating plastic strain effects based on the concept of a modified Weibull stress, $\tilde{\sigma}_w$. The presentation begins with descriptions of the experimental fracture testing conducted on three-point bend specimens with varying geometries for typical pressure vessel grade steels. Attention is then directed to calibration of the Weibull stress parameters for the two pressure vessel steels using the measured toughness distributions of J_c-values for deep and shallow SE(B) specimens.

The section concludes with applications of the Weibull stress methodology to predict the geometry dependence of J_c-values using the toughness values for subsize (PCVN) configurations.

3.1. Specimen geometry effects on J_c-values for pressure vessel steels

Ruggieri et al. [7] performed a series of fracture toughness tests in the T-L orientation on conventional, plane-sided three-point bend fracture specimens with $a/W = 0.15$ and $a/W = 0.5$, $B = 30$ mm, $W = 60$ mm and $S = 4W$. Fracture tests were also performed on plane-sided, precracked Charpy (PCVN) specimen with $a/W = 0.5$, $B = 10$ mm, $W = 10$ mm and $S = 4W$. Here, the tested material is a typical ASTM A515 Grade 65 [60] pressure vessel steel with 294 MPa yield stress also having high strain hardening behavior ($\sigma_{uts}/\sigma_{ys} \approx 1.7 \sim 1.8$). Testing of these fracture specimens was conducted in the DBT region for the tested material (see further details in Ruggieri et al. [7]) at different low temperatures, defined by $T = -10\,^{\circ}$C for the deeply-cracked SE(B) specimen and PCVN configuration with $a/W = 0.5$ and $T = -20\,^{\circ}$C for the shallow crack SE(B) specimen with $a/W = 0.2$.

In related work, Savioli and Ruggieri [61] also report fracture toughness tests on three-point bend fracture specimens with varying crack sizes and specimen thickness in the T-L orientation. The material utilized in their study is a typical ASTM A285 Grade C [62] pressure vessel steel with 230 MPa yield stress and high strain hardening behavior with $\sigma_{uts}/\sigma_{ys} \approx 2$ at room temperature ($T = 20^{\circ}$C); here, σ_{ys} is the yield stress and σ_{uts} represents the tensile strength. The fracture mechanics tests include: (1) conventional, plane-sided 1T SE(B) specimens with $a/W = 0.2$ and $a/W = 0.5$ $B = 25$ mm, $W = 50$ mm and $S = 4W$, and (2) plane-sided, precracked Charpy specimens with $a/W = 0.5$, $B = 10$ mm, $W = 10$ mm and $S = 4W$. ASTM E1820 [63] also provides additional details for the geometry and dimensions of the tested fracture specimens. Testing of these configurations was performed at $T = -80\,^{\circ}$C for the deeply-cracked SE(B) specimen and PCVN configuration with $a/W = 0.5$ and at $T = -60\,^{\circ}$C for the shallow crack SE(B) specimen with $a/W = 0.2$; these temperatures correspond to the lower-shelf, ductile-to-brittle transition behavior for the tested steel (refer to Savioli and Ruggieri [61]).

In the above experimental studies, records of load vs. crack mouth opening displacements (CMOD) were obtained for each specimen using a clip gage mounted on an integrated knife-edge machined into the notch mouth. Cleavage fracture toughness values, characterized in terms of a single toughness measure at fracture instability (J_c), are evaluated from the plastic area under the load-CMOD curve and then using the estimation procedure given in ASTM E1820 [63] based on plastic η-factors. Post-mortem examination of the fracture surfaces for all tested specimens reported by Savioli and Ruggieri [61] and Ruggieri et al. [7] revealed essentially no ductile tearing prior to cleavage fracture thereby providing strong support to the Weibull stress analysis for the tested materials described later.

Fig. 2(a) and (b) display the cumulative Weibull distribution of toughness values for the tested specimens and both materials in which the solid symbols in the plots represent the experimentally measured fracture toughness (J_c)-values. Values of cumulative probability, $F(J_c)$, are obtained by ordering the J_c-values and using the median rank position defined in terms of $F(J_{c,k}) = (k - 0.3)/(N + 0.4)$, where k denotes the rank number and N defines the total number of experimental toughness values [53]. The fitting curves to the experimental data shown in this figure describe the three-parameter Weibull distribution [53] for J_c-values given by

$$F(J_c) = 1 - \exp\left[-\left(\frac{J_c - J_{\min}}{J_0 - J_{\min}}\right)^{\alpha}\right] \tag{8}$$

in which α defines the Weibull modulus (which characterizes the scatter in test data), J_0 is the characteristic toughness and $J_{\min}$ denotes the threshold J-value corresponding to a $K_{\min}$ of 20 MPa$\sqrt{\text{m}}$. In the above, the Weibull modulus often takes the value $\alpha = 2$ to describe the distribution of J_c-values under well-contained near-tip plasticity - this makes contact with the probabilistic treatment of fracture under SSY conditions based upon weakest link statistics [31] and also with the Master Curve methodology given by ASTM E1921 [64]. As expected, there is a relatively marked increase in fracture toughness values for the shallow crack SE(B) specimen and the plane-sided PCVN configuration compared with the characteristic toughness for the deeply-cracked SE(B) geometry. In particular, the PCVN specimen with $a/W = 0.5$ and $W = B$ geometry displays significant elevation in fracture toughness relative to the 1T deeply-cracked SE(B) specimen ($a/W = 0.5$) with $W = 2B$ geometry thereby underlying the loss of crack-tip constraint coupled with a pronounced absolute size/thickness effect exhibited by this crack configuration.

The toughness scaling procedure adopted next in Section 3.2 enables the correction of the statistical distribution for fracture toughness data measured from two sets of test specimens exhibiting widely different characteristic toughness, J_0. Since this parameter plays a key role in the Weibull stress parameter calibration and the constraint correction of toughness, it is of interest to inquire to what extent the quality of fitting affects the estimated value of parameter J_0. To address this issue, Ruggieri et al. [7] conducted a standard maximum likelihood (ML) estimation procedure [53] to determine *both* α and J_0 of the J_c-distribution for the tested A515 pressure steel considered in their work. That analysis reveals that, while the Weibull modulus does change (with respect to the fixed value of $\alpha = 2$) to reflect a different data scatter, the estimated J_0-value displays little sensitivity to the α-value. Indeed, they show that differences in J_0-estimates are $\approx 5\%$ for the tested deeply-cracked geometries and only $\approx 1\%$ for the tested shallow crack specimens. These results strongly suggest that the degree of accord between the experimental data and the Weibull distribution described by Eq. (8) has little effect on cleavage fracture predictions based on the toughness scaling procedure using the correction of J_0-values addressed next.

3.2. Calibration of Weibull stress parameters

The Weibull stress methodology outlined above requires correct specification of the m-value to provide accurate fracture toughness predictions. Further, the function Ψ_c also represents a requisite parameter entering directly into the calculation of $\tilde{\sigma}_w$ through Eq. (7). This section addresses essential features of the calibration procedure to determine the Weibull stress parameters for the two pressure vessel steels described before. Because the focus of the present study is on the prediction of specimen geometry effects on J_c-values using the toughness distribution for subsize (PCVN) configurations, parameters m and Ψ_c are calibrated using the standard SE(B) specimens having a deep and shallow crack for both tested steels.

The calibration strategy relies directly on the toughness scaling model (TSM) building upon previous work of Gao et al. [32] and more recently upon the work of Ruggieri et al. [7] and Ruggieri [65]. Here, we follow these latter works closely and provide only the salient results of the calibration process. Readers are referred to those studies for a full account of the calibration procedure and calibrated parameters for the two tested materials. In all analyses, the research code WSTRESS [66] is utilized to compute the Weibull stress trajectories and to calibrate the Weibull modulus, m for the tested steels based on the standard Beremin model (*i.e.*, $\Psi_c = 1$ as already noted).

We begin by following similar arguments to those given by R&D [6] to define the fraction of fractured particles as a two-parameter Weibull distribution given by Wallin and Laukkanen [29] as

$$\Psi_c = 1 - \exp\left[-\left(\frac{\sigma_{pf}}{\sigma_{prs}}\right)^{\alpha_p}\right] \tag{9}$$

where σ_{prs} is the particle reference fracture stress, α_p denotes the Weibull modulus of the particle fracture stress distribution and $\sigma_{pf} = \sqrt{1.3\sigma_1\epsilon_p E_d}$ characterizes the particle fracture stress in which σ_1 is the maximum principal stress, ϵ_p denotes the effective matrix plastic strain and E_d represents the particle's elastic modulus. Here, it is understood that the particle reference stress, σ_{prs}, represents an approximate average for the distribution of the particle fracture stress. For ferritic structural steels, such as the pressure vessel materials utilized in this study, typical values of α_p and E_d are 4 and 400 GPa as reported by Wallin and Laukkanen [29]; these values are employed in the present analyses.

With the fraction of fracture particles thus defined, consider first the fracture toughness data for the A515 steel previously described. Here, calibration of parameter m is conducted at the test temperature, $T = -10\,^{\circ}\text{C}$, by scaling the characteristic toughness of the measured toughness distribution for the shallow crack SE(B) specimen with $a/W = 0.15$ to the equivalent characteristic toughness of the toughness distribution for the deeply-cracked SE(B) specimen with $a/W = 0.5$. However, because the specimens were not tested at the same temperature, the present methodology adopts a simple procedure to correct the measured toughness values for temperature using the Master Curve methodology described in ASTM E1921 [64] leading to a toughness ratio of $J^{a/W=0.15}_{SE(B)}/J^{a/W=0.5}_{SE(B)} \sim 1.4$ at $T = -10\,^{\circ}\text{C}$. The calibrated Weibull modulus then yields a value of $m_0 = 11$ which is well within the range of previously reported m-values for common pressure vessel and structural steels (see, *e.g.*, [1,4,32,5,67]. Fig. 3(a) display the $\tilde{\sigma}_w$ vs. J trajectories based on the standard Beremin model with $m_0 = 11$ for both specimen geometries at the test temperature, $T = -10\,^{\circ}\text{C}$ and the associated toughness corrections; in these plots, $\tilde{\sigma}_w$ is normalized by the material yield stress, σ_{ys}. Calibration of the function Ψ_c in previous Eq. (9) then follows from determining parameter σ_{prs} that gives the best correction of measured toughness values at $T = -10\,^{\circ}\text{C}$ for the shallow and deep crack SE(B) specimens with a fixed value $m_0 = 11$. Fig. 3(b) provides the constraint correlations ($J^{a/W=0.15}_{SE(B)} \rightarrow J^{a/W=0.5}_{SE(B)}$) for varying

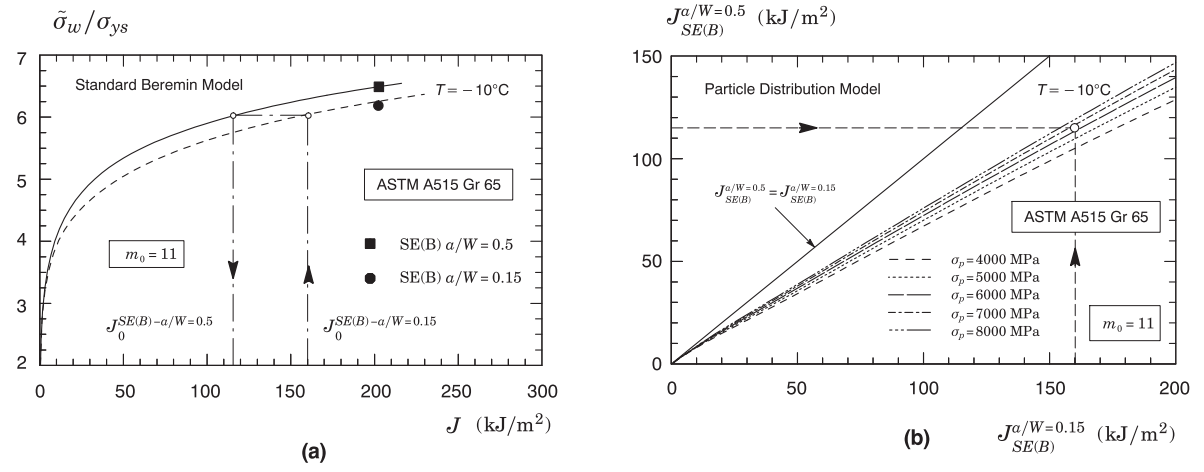

Fig. 3. Calibration of Weibull stress parameters for the tested A515 steel: (a) $\tilde{\sigma}_w$ vs. J trajectories for the shallow and deeply-cracked SE(B) specimens at $T = -10\,^{\circ}\text{C}$ based on the standard Beremin model with $m_0 = 11$; (b) Constraint correlations of J-values at $T = -10\,^{\circ}\text{C}$ for $m_0 = 11$ and the simplified particle distribution (WL) model with varying σ_{prs}-values.

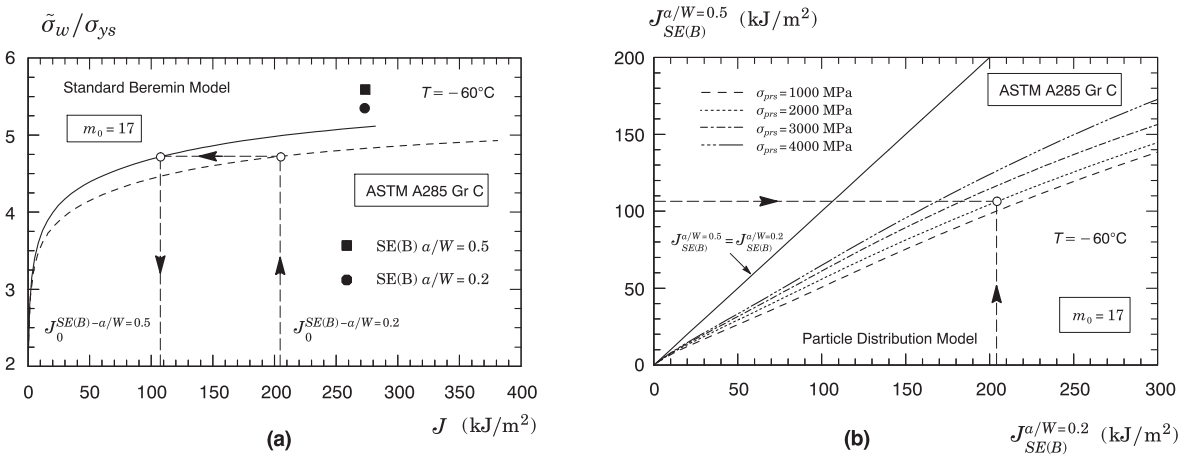

Fig. 4. Calibration of Weibull stress parameters for the tested A285 steel: (a) $\tilde{\sigma}_w$ vs. J trajectories for the shallow and deeply-cracked SE(B) specimens at $T = -160$ °C based on the standard Beremin model with $m_0 = 17$; (b) Constraint correlations of J-values at $T = -60$ °C for $m_0 = 17$ and the simplified particle distribution (WL) model with varying σ_{prs}-values.

values of parameter σ_{prs} from which the best value of particle fracture stress that corrects the characteristic toughness for the shallow crack SE(B) specimen, $J_0^{SE(B)-a/W=0.15}$, to its equivalent characteristic toughness for the deeply-cracked SE(B) specimen, $J_0^{SE(B)-a/W=0.5}$, is given by $\sigma_{prs} = 6500$ MPa.

Now direct attention to the fracture toughness data for the A285 steel shown in previous section. The calibration procedure of parameters m and Ψ_c repeats the two-step procedure already outlined. In the present application, calibration of parameter m is conducted at the test temperature, $T = -60$ °C , by scaling the characteristic toughness of the measured toughness distribution for the shallow crack SE(B) geometry with $a/W = 0.2$ to the equivalent J_0-value for the deeply-cracked SE(B) specimen with $a/W = 0.5$ using again the Master Curve methodology [64] thereby yielding a toughness ratio of $J_{SE(B)}^{a/W=0.2}/J_{SE(B)}^{a/W=0.5} \sim 1.9$ at $T = -60$ °C. Using now the TSM to correct the characteristic toughness for the shallow crack SE(B) geometry, $J_0^{SE(B)-a/W=0.2}$, to its equivalent characteristic toughness for the deeply-cracked SE(B) specimen, $J_0^{SE(B)-a/W=0.5}$, the calibrated Weibull modulus then yields a value of $m_0 = 17$ which is also well within the range of previously reported m-values for common pressure vessel and structural steels (see, *e.g.*, [1,4,32,31,5,67]. Fig. 4(a) displays the evolution of $\tilde{\sigma}_w$ normalized by the material yield stress, σ_{ys}, with increased J-values based on the standard Beremin model with $m_0 = 17$ for both specimen geometries at the test temperature, $T = -60$ °C. Having determined the Weibull modulus, m, calibration of the function Ψ_c proceeds by evaluation of parameter σ_{prs} that gives the best correction of measured toughness values at $T = -60$ °C for the deeply-cracked SE(B) specimen and the shallow crack SE(B) geometry with $a/W = 0.2$ with a fixed value $m_0 = 17$. To illustrate the calibration process, Fig. 4(b) provides the constraint correlations ($J_{SE(B)}^{a/W=0.5} \rightarrow J_{SE(B)}^{a/W=0.2}$) for varying values of parameters σ_{prs} while holding fixed $\alpha_p = 4$ and $E_d = 400$ GPa. Here, correction of the characteristic toughness for the shallow crack SE(B) geometry, $J_0^{SE(B)-a/W=0.2}$, to its equivalent characteristic toughness for the deeply-cracked SE(B) specimen, $J_0^{SE(B)-a/W=0.5}$, then yields $\sigma_{prs} = 2000$ MPa for the tested A285 steel.

3.3. Multiscale predictions of fracture toughness

To verify the predictive capability of the modified Weibull stress methodology adopted in the present work, this section describes applications of the $\tilde{\sigma}_w$-based approach to predict effects of geometry and constraint loss on cleavage fracture toughness values (J_c) for the two tested pressure vessel steels. We also follow the works of Ruggieri et al. [7] and Ruggieri [65] closely here in which primary attention is given to results pertaining to predictions of the measured distribution of cleavage fracture values for the deeply-cracked SE(B) specimen using the measured fracture toughness distribution for the PCVN geometry. The correlative procedure to obtain the toughness correction $J_0^{PCVN} \rightarrow J_0^{SE(B)-a/W=0.5}$ follows similar protocol for the toughness scaling methodology outlined previously. As already noted, the calibrated Weibull modulus is assumed as a material property at temperatures within the DBT region and sufficiently close to the test temperature.

Figs. 5 and 6 show the Weibull cumulative distribution function of J_c-values for the SE(B) specimen with $a/W = 0.5$ predicted from the experimental fracture toughness distribution for the PCVN configuration for the materials under discussion. These plots include fracture predictions based on the modified Weibull stress model incorporating the simplified particle distribution with the calibrated σ_{prs}-value and on the standard Beremin model. The solid lines in these plots represents the prediction of the median fracture probability whereas the dashed lines in Fig. 5 define the 90% confidence limits

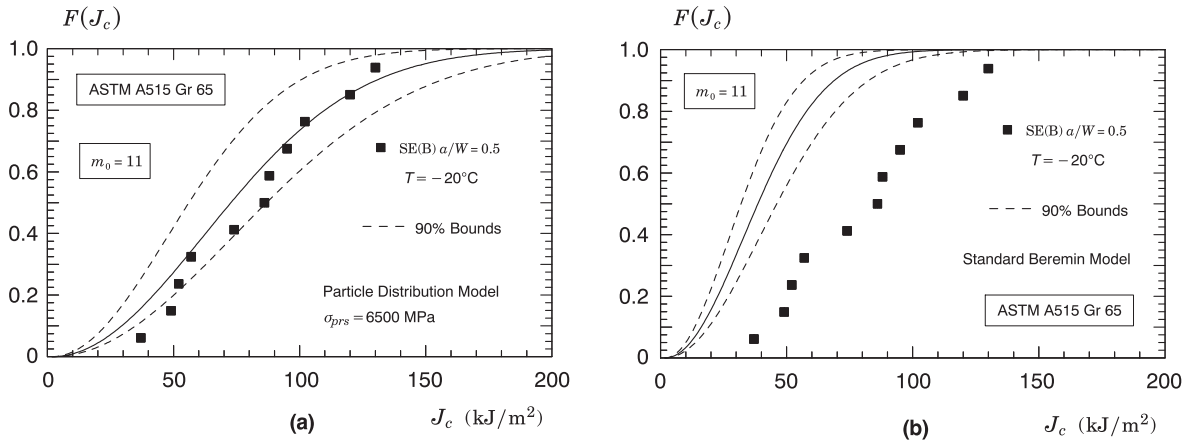

Fig. 5. Predicted cumulative Weibull distribution of experimentally measured J_c-values and 90% confidence bounds for the SE(B) specimen with $a/W = 0.5$ for the tested A515 steel at $T = -20$ °C: (a) Simplified particle distribution model with $\sigma_{prs} = 6500$ MPa and $m_0 = 11$; (b) Standard Beremin model with $m_0 = 11$.

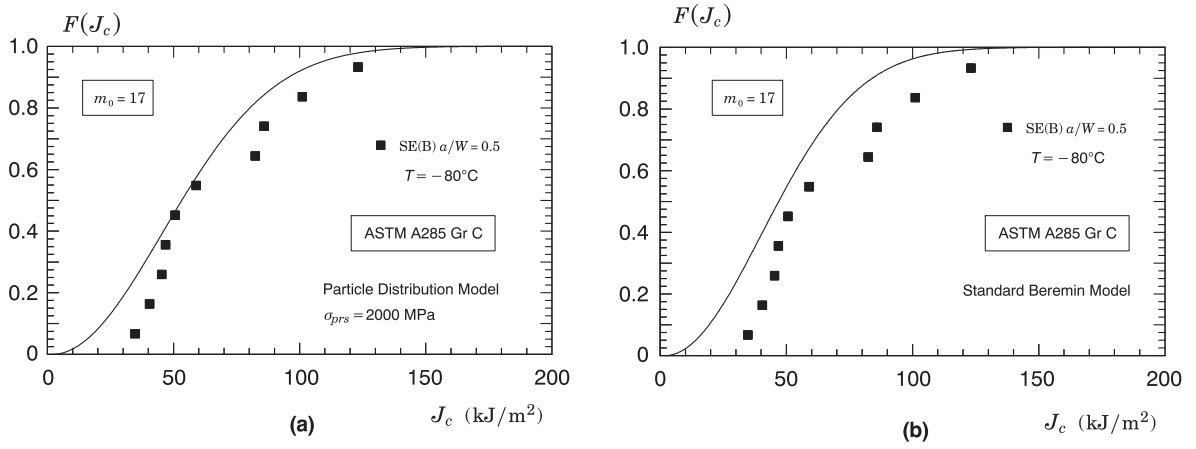

Fig. 6. Predicted cumulative Weibull distribution of experimentally measured J_c-values for the SE(B) specimen with $a/W = 0.5$ for the tested A285 steel at $T = -80$ °C: (a) Simplified particle distribution model with $\sigma_{prs} = 2000$ MPa and $m_0 = 17$; (b) Standard Beremin model with $m_0 = 17$.

obtained from using the 90% confidence bounds for J_0 [68,53,7]. The figures also include the experimentally measured fracture toughness (J_c)-values for the tested specimens and materials.

For the A515 steel, the predicted Weibull distribution derived from the simplified particle distribution displayed in Fig. 5 (a) agrees well with the experimental data; here, most of the measured J_c-values lie within the 90% confidence bounds. In contrast, the predicted Weibull cumulative distribution based on the standard Beremin model, including the 90% confidence bounds, is entirely shifted to the left of the experimental data thereby providing conservative estimates of fracture toughness for the deeply-cracked SE(B) specimen.

Similar trends are observed for the results corresponding to the A285 steel. The predicted distribution for the 1T SE(B) specimen derived from the simplified particle distribution shown in Fig. 6(a) exhibits good agreement with the experimental data. While most of the measured J_c-values lie slightly outside the median distribution, the predictions nevertheless provide close description of the measured toughness distribution for the deeply-cracked bend specimen. Now direct attention to the predicted Weibull distribution derived from the standard Beremin model displayed in Fig. 6(b). Here, the predicted Weibull cumulative distribution is entirely shifted to the left of the experimental data, albeit also in reasonable agreement with the measured J_c-values, thereby providing a somewhat more conservative estimate of fracture toughness values for the 1T SE(B) specimen.

4. Robustness of the Weibull stress approach: pertinent features

The introduction of a rational and tractable probabilistic framework to describe the essential features of the cleavage fracture micromechanism in connection with its random nature extends conventional (phenomenological) fracture

mechanics methodology and enables the development of convenient procedures to predict the effects of constraint variations on measured values of fracture toughness while, at the same time, allowing estimation of the failure probability for cracked structural components. However, while the LAF methodologies outlined in previous sections have proven sufficiently effective to serve as a basis for multiscale predictions of fracture toughness, there still remain some issues that can have important practical implications for robustness of the probabilistic model based on the Weibull stress concept.

Most of the studies thus far have essentially focused on the application of LAF methodologies, including specifically the Beremin model, to describe and predict cleavage fracture toughness in structural steels based on limited experimental data. Since the Weibull stress parameters simply reflect the random nature of cleavage fracture and are, thus, strongly dependent on the micro features of the material, it is natural to raise the question as to what extent the often large variability in experimentally measured toughness values coupled with details associated with finite element modeling, including mesh refinement, affect the predictive response of the Weibull stress approach. Moreover, in using the probabilistic methodology and the results outlined previously, it is well to keep in mind that the Weibull stress parameters should possess the following key features: (1) they should be easily obtainable from limited experimental data with only modest calibration effort required; (2) they should correspond as close as possible to the actual micromechanics features of the underlying cleavage process; (3) they should be broadly applicable to describe and predict cleavage fracture behavior across different structural crack configurations and loading conditions. Undoubtedly, the first issue related to the accurate and robust calibration of the Weibull stress parameters, specifically with regard to the Weibull modulus defined by parameter m, appears to be the most critical one. Here, we provide a critical discussion of the central features related to the robustness of the Weibull stress approach.

4.1. Parameter calibration

Previously developed procedures to calibrate the Weibull parameters, (see [4,31] for additional details) employ toughness data for cleavage fracture (such as J_c-values) measured from only one set of specimens. These toughness measures form the basis upon which an iterative procedure incorporating a standard statistical method (such as the maximum likelihood method [53]) provides parameters m and σ_u. However, Gao et al. [32] and later Ruggieri et al. [69] have shown that such a methodology based on a single set of specimens provides nonunique parameters, *i.e.*, many pairs of (m, σ_u) provide equal correlations of critical Weibull stress values with the measured distribution of toughness data. Gao et al. [32] have further advanced the calibration procedure to introduce an improved methodology that employs a toughness scaling model based upon the Weibull stress to determine parameter m based upon fracture toughness data measured from two sets of specimens spanning a wide range of crack-tip constraint (triaxiality). By using the Weibull stress trajectories for two crack configurations exhibiting different constraint levels (*e.g.,* a deep notch and a shallow notch SE(B) specimen), the process seeks the m-value which corrects the corresponding measured toughness distributions thereby eliminating the non-uniqueness of calibrated Weibull stress parameters that arises when using only one set of fracture toughness.

However, while the Gao et al. approach has proven highly effective in predictions of cleavage fracture toughness for several structural steels tested in the DBT region (see, *e.g.*, the representative works of Gao et al. [70], Gao and Dodds [71,72], Petti and Dodds [73,33], Ruggieri [5,34] and R&D [6,7]), it does require fracture testing of different crack configurations and/or specimen geometries. Routine fracture assessments of structural components typically employ limited testing of small material samples using only standard fracture specimens (such as deeply notched C(T) or SE(B) specimens) which can make calibrations of the Weibull stress parameters using two sets of specimens all but very demanding and rather cumbersome, if not prohibitive in several cases. Moreover, difficulties still persist in performing the calibration procedure for use in engineering analysis to obtain parameters, more specifically the Weibull modulus, which are reasonably invariant to the specimen configurations used in this two-set approach. For example, the analyses conducted in previous Section 3 employed the toughness distributions for standard SE(B) specimens having a deep and shallow crack to calibrate parameter m and σ_{prs} for both tested pressure vessel steels and then to predict the toughness distribution for the PCVN geometry. It is natural to raise the question as to whether using fracture toughness data measured from two other different sets of specimens would yield reasonably close calibrated parameters. For the cases under discussion, employing the toughness distributions for standard deeply cracked SE(B) specimens and the PCVN geometry to calibrate parameter m and σ_{prs} would still provide a good prediction of the toughness distribution for the shallow crack SE(B) specimens. However, the collective evidence at present from a wide range of researchers reveals an uncertain picture of the calibration process; some studies obtain similar m-values for different specimen types while others show surprisingly large differences. Reported values of m for common structural and pressure vessel steels range from 10 to 50.

When the modified Weibull stress approach incorporating plastic strain effects described earlier is employed, this picture becomes even more complicated as the model now requires specification of a second parameter describing the fraction of Griffith-like microcracks which are eligible to propagate unstably. For a given material under specified conditions, the calibration procedure adopted by Ruggieri et al.[7] and Ruggieri [65] does provide a viable basis for structural integrity applications once adequate fracture toughness values measured from two sets of test specimens. However, more robust and yet simpler schemes to calibrate the parameters (m, σ_u) clearly become necessary in routine engineering analyses as there is much to improve on the calibration strategy for the Weibull stress parameters.

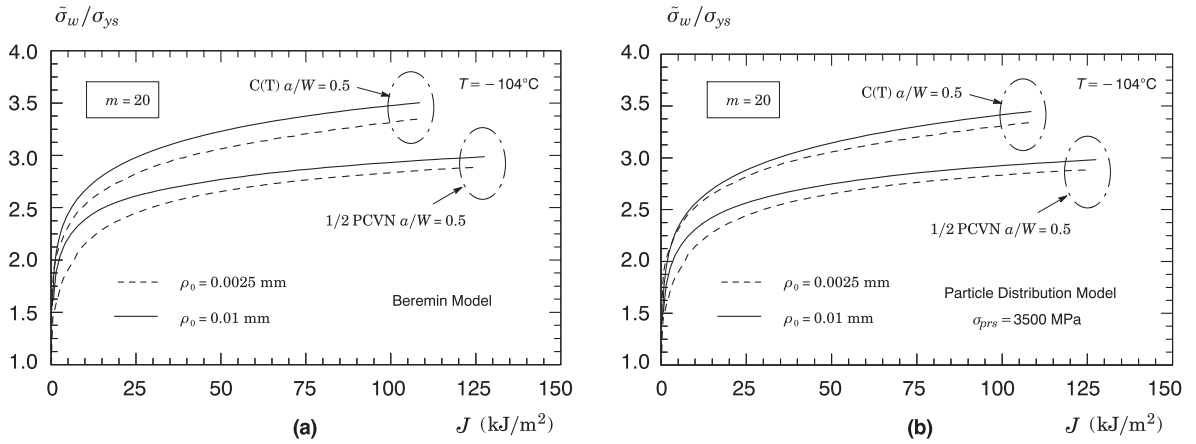

Fig. 7. Effect of blunt notch size, ρ_0, on $\tilde{\sigma}_w$-trajectories for the 1T C(T) specimen with $a/W = 0.5$ and the deeply-cracked PCVN geometry with $B = 5$ mm made of an A533 Gr B material [74]: (a) Standard Beremin model. (b) Simplified particle distribution model.

4.2. Mesh dependency effects

Since finite element modeling details, including mesh refinement, may affect the predictive response of the Weibull stress approach, it is important to obtain nearly invariant values of the Weibull stress at a fixed, specified macroscopic loading (as characterized by J) is to generate converged numerical descriptions of the crack-tip stress fields which are accurate over distances of order a few CTODs. A weak, implicit length-scale enters the finite element computations through the near-tip mesh size. For example, insufficient mesh refinement reduces peak stress values ahead of the crack front, especially at smaller load levels, thereby strongly affecting the compute values of the Weibull stress calculation since this parameter involves the principal stress raised to a large power defined by the Weibull modulus. In general, extensive element distortion near the notch root prevents numerical convergence at higher J-values when too small notch root radii are used thereby requiring somewhat larger initial root radii to generate numerical solutions over the complete loading history for the analyzed fracture specimens of interest.

To illustrate this issue, consider the $\tilde{\sigma}_w$-trajectories shown in Fig. 7 for two different blunt notch sizes, $\rho_0 = 0.0025$ mm and $\rho_0 = 0.01$ mm derived from numerical solutions for a deeply-cracked C(T) specimen and $1/2$ PCVN geometry, both corresponding to the A533 Gr B material [74]. These analyses generate $\tilde{\sigma}_w$-values for the standard Beremin model and for the simplified particle distribution model with $m = 20$ and $\sigma_{prs} = 3500$ MPa . The material properties are those for the test temperature of $T = -100\,^{\circ}$C with $\sigma_{ys} = 611$ MPa, $E = 207$ GPa and $\nu = 0.3$ reported by Rathbun et al. [75]. As could be expected, the $\tilde{\sigma}_w$-trajectories display some sensitivity to the blunt notch size but which has nevertheless essentially no significant effect on the relative position of the curves, particularly for the simplified particle model shown in Fig. 7(b). Indeed, this is an important point to be made in the present discussion. Since the fracture toughness constraint corrections, $J_{PCVN} \rightarrow J_{C(T)}$, adopted in correlative analyses rely on the $\tilde{\sigma}_w$-trajectories for *both* specimen geometries, small relative changes in *both* $\tilde{\sigma}_w$-curves have only a small effect on fracture predictions.

4.3. Fracture assessments of large structural components

In general, the Weibull stress methodology should enable accurate fracture toughness predictions with reasonable effort over a broad range of geometries and loading conditions. However, because of the rather strong sensitivity of the Weibull stress trajectories forming the toughness scaling methodology and, further, the sensitivity of parameter m on analysis details, including the statistical distribution of measured fracture toughness values, it may no longer be the case that accurate predictions of fracture behavior for larger in-service structures are easily obtainable. Perhaps more importantly, when the methodology is used to estimate an adequate fracture toughness value entering a FFS analysis of a larger structural component such as, for example, a welded beam to beam connection having a surface flaw under predominantly tensile loading, the degree of conservatism is generally unknown.

Since obvious (and great) importance attaches to the predictive capability of the Weibull stress approach to assess the cracking behavior of large structures under low constraint conditions, it is of great interest to ask what are the actual safety margins involved and how the sensitivity of fracture toughness predictions affects its remaining service life. Matos and Dodds [76] first attempted a direct use of the Weibull stress model, coupled with 3-D analyses of beam-column connections containing crack-like defects, to provide a quantitative estimate of the cumulative failure probabilities with increasing beam moment. Following the great Kobe earthquake [77], development and extensions of the Weibull stress model for fracture assessments of beam-to-column joints under seismic conditions and subjected to cyclic and dynamic loading have been

actively pursued by Japanese researchers. In particular, Minami and co-workers [78–88] systematically addressed fracture assessments of steel components under seismic conditions and obtained an engineering procedure for CTOD toughness corrections for constraint loss based on the Weibull stress concept. However, despite these research initiatives, relatively little effort has been expended in validation studies to extend the Weibull stress methodology to fracture assessments of large structural components.

4.4. Loading rate effects

A variety of engineering structures, including marine, aeronautical and civil structural components, operate in dynamic environments subjected to dynamic loads from several different sources. Because the fracture performance of low-to-moderate strength structural steels is strongly sensitive to load rate effects, defect assessments of engineering structures under dynamic loading must consider the effects of strain rate on fracture toughness and, consequently, on the structural integrity. Moreover, nearly all steels show an increase in yield strength with loading rate in which the dynamic yield strength is inversely proportional to absolute temperature and is logarithmically related to the strain rate, $\dot{\epsilon}$. Thus, the Weibull stress concept and its interpretation as a macroscopic crack driving force give a route to incorporate in a proper and yet simple way loading rate effects into multiscale predictions of fracture across different geometries and loading conditions.

Early exploratory work to address loading rate effects on fracture based on the Weibull stress methodology was conducted by Gao et al. [89,90] who examined the potential influence of strain rate on the Weibull stress parameters for an A515 Gr 70 steel tested in the DBT region. Using fracture toughness values for deep and shallow notch specimens derived from both static and dynamic fracture tests, they identified an m-value (Weibull modulus) approximately independent of loading rate thereby indicating that dynamic fracture predictions could be made solely on the basis of changes of parameter σ_u with strain rate. While these research efforts provide analysis of dynamic fracture predictions which seem consistent with the present level of development of the Weibull stress model and is, therefore, to be encouraged in engineering applications, a number of unresolved questions also need to be addressed. For example, since parameter m is related to the microcrack distribution that triggers cleavage fracture, it should expected that the Weibull modulus should also depend on strain rate. For low-to-moderate loading rates, Gao et al. [90,89] found the m-value for the tested steel almost invariant to strain rate but without drawing any definite conclusions about the broad validity of such an approach. For higher loading rates and for more complex dynamic loading, extensions of the Weibull stress methodology remain rather untested as does its development into a systematic framework to couple statistical and dynamic effects on cleavage fracture toughness in the DBT region.

4.5. Materials with macroscopic heterogeneities

The effects of macroscopic heterogeneities on fracture behavior play an important role in accurate assessments of structural integrity for a wide range of engineering structures, including welded components. In particular, reduced fracture performance of a weld joint (as compared to the baseplate material) generally imposes the use of weldments with weld metal strength higher than the baseplate strength, a condition referred to as overmatching, to shield the welded region by shifting the large plastic deformation field into the lower strength baseplate where the fracture resistance is presumably higher and potentially fewer defects occur. However, while the overmatch practice has been used effectively in many structural applications, the level of mismatch between the weld metal and baseplate material may strongly alter the relationship between remotely applied loading and crack-tip driving forces. Here, the interaction between the local crack-tip fields (most often controlled by the flow properties of the weld metal) and the global elastic-plastic regime gives rise to near-tip constraint states which can differ significantly than the corresponding levels in crack-tip constraint for a homogeneous fracture specimen at the same (macroscopic) loading. Moreover, fracture tests of weld specimens exhibit significant scatter in measured values of cleavage fracture toughness caused not only by the variability in the microestructural features of the material but also by macroscopic heterogeneities inherently present along the crack front (see, *e.g.*, Satoh et al. [91] and McGrath and Braid [92]). This phenomenon is further magnified by the overmatching condition in steel weldments thereby contributing to potentially increase the propensity to trigger cleavage before gross yield section. Clearly, the transferability of fracture toughness data measured using small, laboratory specimens to large, complex structural components still remains one of the key difficulties in developments of predictive methodologies for defect assessments of welded structures. Advanced procedures for structural integrity analyses must include the complex interplay between the effects of weld strength mismatch and the variability of cleavage resistance at the microstructural level for the different regions of steel weldments.

To address this issue on the basis of a probabilistic framework, the Weibull stress approach can easily be extended in a rather simplified manner to consider typical weld crack configurations. Consider first a schematic illustration of a macroscopic crack embedded in the weld metal depicted in Fig. 8(a) in which the fracture process zone is fully confined to the weld material. Since fracture takes place entirely in the weld metal, the distribution of cleavage fracture stress can expressed as the two-parameter Weibull function in terms of σ_w or, in a more general form, by $\bar{\sigma}_w$ described by previous Eqs. (3) and (6) [34]. Observe, however, that the Weibull stress parameters (m, σ_u) are related to the weld metal properties, including fracture toughness, flow properties and the level of weld strength mismatch, and should be calibrated accordingly based on the procedure described in Gao et al. [32] but using weld fracture specimens having shallow and deep cracks.

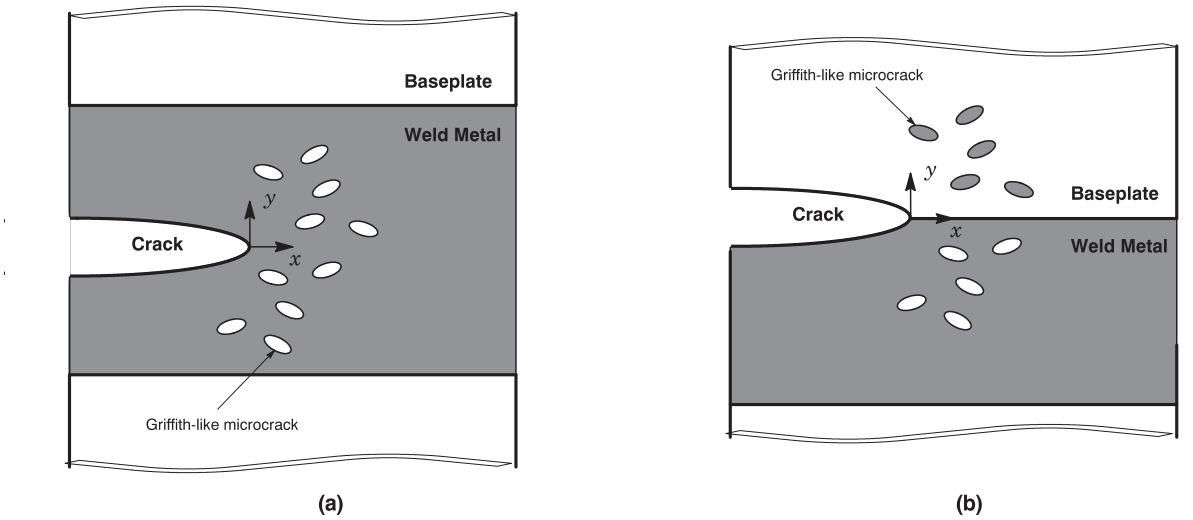

Fig. 8. (a) Schematic of a macroscopic crack embedded in the weld metal in which the fracture process zone is fully confined to the weld material. (b) Interface macroscopic face between the weld metal and baseplate material.

Consider now a bimaterial crack configuration shown in Fig. 8(b), which represents a macroscopic crack at the interface between the weld metal and the baseplate material (the heat affected zone is not considered for simplicity). Upon loading (and crack opening), cleavage fracture can occur either in the weld metal or in the baseplate material so that one is tempted to adopt a mixed distribution model such that the k-folded probability density function is given by [53]

$$f_X(x) = \sum_{k=1}^{r} p_k f_{X_{k(x)}} \tag{10}$$

where $f_{X_k}(x)$ is the k-th subpopulation and $0 \leqslant p_k \leq 1$ in which p_k is often referred to as the mixing parameter [53]. With cleavage fracture toughness conveniently described by a Weibull distribution (let us assume a two-parameter distribution for convenience), then a twofold mixed Weibull distribution describing cleavage fracture toughness, as characterized by J_c, could be of the form

$$F_X(J_c) = p\left[1 - \exp\left(\frac{J_c}{\beta_{WM}}\right)^{\alpha_{WM}}\right] + (1-p)\left[1 - \exp\left(\frac{J_c}{\beta_{BM}}\right)^{\alpha_{BM}}\right] \tag{11}$$

where α_{WM}, α_{BM}, β_{WM} and β_{BM} are parameters of the Weibull distribution with WM and BM denoting the weld metal and the baseplate material. The above expression then motivates introducing analogously a twofold mixed Weibull stress distribution for the cleavage fracture stress given by

$$P_f(\tilde{\sigma}_w) = p\left\{1 - \exp\left[-\left(\frac{\tilde{\sigma}_w}{\sigma_{u,WM}}\right)^{m_{WM}}\right]\right\} + (1-p)\left\{1 - \exp\left[-\left(\frac{\tilde{\sigma}_w}{\sigma_{u,BM}}\right)^{m_{BM}}\right]\right\} \quad . \tag{12}$$

The resulting twofold mixed Weibull stress distribution is rather complex to manipulate in general since it requires the specification of two sets of Weibull stress parameters (one for each material) and the mixing parameter p. Clearly, for engineering applications, the calibration procedure to specify values for the Weibull stress parameters remains a non-trivial task in connection with the enormous testing demands to obtain a representative set of experimental toughness values describing the interface crack problem.

4.6. The weakest link paradigm

At the heart of LAF models to describe cleavage fracture in ferritic steels, including the Beremin model and the modified Weibull stress approach outlined in the present work, is the weakest link statistics related to the distribution of the largest and most favorably oriented, fractured carbides (here associated with the Griffith-like microcracks) embedded in the near-tip highly stressed region. While often overlooked in applications of LAF models to cleavage fracture, the weakest link concept represents a key central assumption in the development of the probabilistic model as it strongly relies on the catastrophic failure being controlled by the instability of the weakest flaw, which may not necessarily describe the local fracture mechanism. Further, another assumption that also plays a central role in developing LAF models to cleavage fracture lies in the adoption of a Griffith criterion to characterize unstable propagation of the largest and most favorably oriented, fractured carbide. Since the Griffith criterion implies linear elastic conditions and, further, since the Griffith-like microcracks

are formed in the course of plastic deformation ahead of the (macroscopic) crack tip, it becomes clear that valid objections can be raised against this assumption.

For materials having local inhomogeneity in strength, the unstable propagation of a flaw may be arrested by the surrounding region having higher fracture resistance. Failure of a critical flaw in any small element of the material causes redistribution of the local stresses, so that increasing the applied load is necessary to promote further cracking. Only after a number of elements have cracked does the failure occur in a macroscopic scale, ultimately through a chain-of-bundles mechanism [93,94]. Brittle fracture preceded by extensive near-tip plastic deformation and intense blunting of the tip, as observed in most steels in the transition region, also bears strong similarity to this mechanism. The local stresses are therefore redistributed to the uncracked near-tip elements until a local critical stress is reached. Fracture is thus locally progressive to the extent that instability of a critical flaw may no longer lead to total failure thereby yielding a limiting distribution for the fracture stress in terms of a first asymptotic distribution of smallest values or Gumbel distribution [53] – observe here that the Weibull distribution describing the fracture stress is defined by a third asymptotic distribution of smallest values [53].

Early research efforts made use of the chain-of-bundles probability model primarily to analyze the strength of fibrous and composite materials [95–98]. However, since both models share commonly the essential features of an asymptotic distribution of smallest values [53] to characterize material failure and, further, since the Gumbel distributions is essentially an extreme value distribution derived from the logarithmic transformation of the two-parameter Weibull function, we confidently expect a good description of cleavage fracture in situations for which the weakest link assumptions are perhaps too stringent.

4.7. Delamination effects on fracture toughness

A case of considerable interest also involves the phenomenon of delamination associated with increased fracture toughness in structural alloys. Here, development of delamination cracking in the transverse ($L-T$ or $T-L$) direction for common fracture specimens affects their macroscopic fracture behavior by changing the crack front (through thickness) constraint and, at the same time, providing an additional contribution to the total work of fracture. Early experimental studies on delamination effects in notch impact specimens for hot-rolled steels [99–101] revealed a marked influence of delamination cracking on the ductile-to-brittle transition (DBT) behavior for these materials as the ductile-brittle transition shifts towards lower temperatures with increased number of fracture surface delaminations. These effects arise from the strong interaction between anisotropic microstructural features of the material which govern the separation of transverse weak planes and the loss of stress triaxiality in the crack front region due to through-thickness splitting. While these previous studies advanced the understanding of delamination effects on the experimental fracture toughness behavior of structural materials, only little effort has been expended to quantify the rather complex interaction of a transverse delamination with the macroscopic crack front. The primary reason offered for the increased fracture toughness observed in fracture testing of specimens in the transverse ($L-T$ or $T-L$) direction is that the behavior of laminated materials is controlled by a mechanism of crack-divider delamination toughening in which the incidence of through-thickness splitting results in loss of through-thickness constraint [102]. However, how the controlling mechanical features - delamination size and crack-tip constraint - are interconnected and their relative contributions to the macroscopic fracture behavior remain open issues.

To address this issue, an exploratory application of the Weibull stress approach provides valuable insight into the effect of delamination cracks on macroscopic fracture behavior in conventional fracture specimens. Alam et al. [103] recently performed fracture toughness tests on conventional, plane-sided three-point bend fracture specimens with $a/W = 0.5$ in the L-T and T-L orientation. The geometry and dimensions of the tested fracture specimens follow ASTM E1820 [63] with $B = 1.67$ mm, $W = 3.33$ mm and $S = 4W$. Here, a is the crack size, W denotes the specimen width, B represents the specimen thickness and S is the load span. Testing of this configuration was performed at different temperatures ranging from $T = 20\,^{\circ}$C to $-196\,^{\circ}$C. The material is a very high strength nanostructured ferritic alloy (NFA) designated as 14YWT ($Fe-14Cr-3W-0.4Ti-0.2Y_2O_3$ wt.%) and developed at Oak Ridge National Laboratory [104] for future fission and fusion reactor critical applications. This class of NFA material is derived from oxide (Y_2O_3) dispersion strengthened (ODS) ferritic alloys with increased amount of chromium and Y_2O_3 which results in excellent fracture toughness properties at low temperatures. The fracture toughness tests of the deeply-cracked SE(B) specimens were performed following the procedures given by ASTM E1921 [64] and ASTM E1820 [63] based on records of load versus load line displacement (LLD). Exceptionally high fracture toughness and low transition temperature were observed by Alam et al. [103] in which the measured upper-shelf fracture toughness is in the range of $K_J = 100\ \mathrm{MPa}\sqrt{\mathrm{m}}$ with a remarkably low ductile-to-brittle transition (DBT) temperature at about $-175\,^{\circ}$C - here, fracture toughness characterized in terms of K_J-values is determined using the standard relationship $J = (1-\nu^2)K_J^2/E$ where E is the elastic longitudinal modulus and ν is Poisson's ratio. Much of this fracture toughness behavior can explained in terms of the connection between delamination cracking and increased toughness due to loss of through-thickness constraint by a crack-divider toughening mechanism where it is evident that the through-thickness splitting causes the bulk of the specimen to be divided into thinner ligaments defined by the delamination cracks thereby relaxing the near-tip stresses which drive the cleavage fracture process and, further, affecting strongly the crack-front size over which high levels of near-tip stress triaxiality (constraint) are maintained.

In recent and yet-unpublished work, Ruggieri et al. [105] conducted extensive set of nonlinear, 3-D finite element analyses of subsize SE(B) fracture specimens with a prescribed crack-divider delamination made of NFA material to describe the

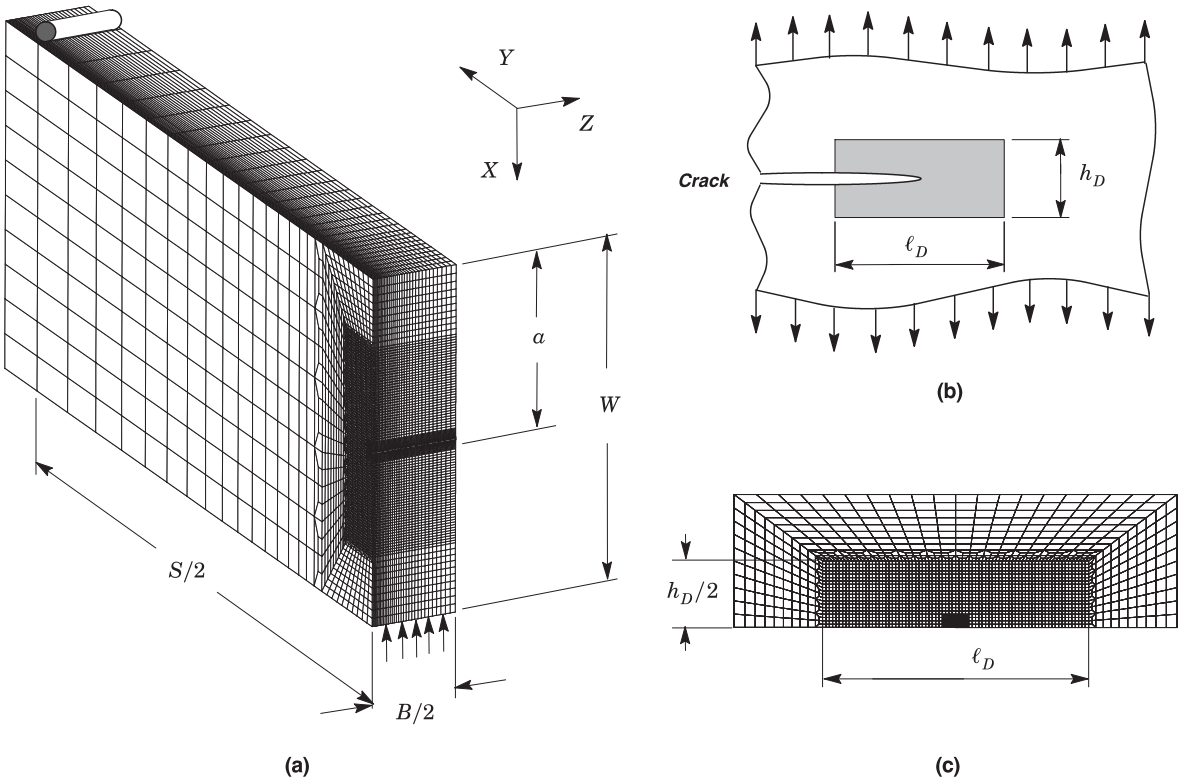

Fig. 9. (a) Quarter-symmetric finite element model used in the 3-D analyses of an SE(B) specimen with $a/W = 0.5$ made of a nanostructured ferritic alloy (NFA) tested by Alam et al. [103]. (b) Schematic for the adopted geometry of the transverse rectangular delamination. (c) Finite element model of the transverse rectangular delamination including the near-tip mesh detail.

coupling effect of specimen geometry and delamination size on fracture behavior based on the Weibull stress as the crack driving force. Here, we follow that work closely and repeat the key results that have a direct bearing on the probabilistic framework pursued in this work. Fig. 9(a) shows the finite element model constructed for analyses of the tested SE(B) specimen. Modeling of the center-plane delamination crack requires a very refined crack-front mesh to adequately characterize the stress-free delamination surface and to resolve accurately the crack-front stress fields. A conventional mesh configuration having a focused ring of elements surrounding the crack front is used with a small blunt notch at the crack tip; the radius of the blunt notch, ρ_0, is 1 μm (0.001 mm). Symmetry conditions enable analyses using one-quarter of the 3-D models with appropriate constraints imposed on the symmetry planes. The finite element mesh has 33 variable thickness layers defined over the half-thickness $(B/2)$ to accommodate strong Z variations in the stress distribution and at the same time to resolve the steep stress gradients near the center-plane delamination crack. Here, the layer thickness defining the delamination crack at $Z = 0$ is $0.006B$ whereas the layer defined near the free surface $(Z = B/2)$ is $0.03B$. The quarter-symmetric, 3-D model for this specimen has 98,702 nodes and 92,037 elements.

Because transverse delamination cracking is associated with anisotropic microstructural features of the material which govern the separation of transverse weak planes [101], a delamination crack in the specimen center-plane region with a prescribed length, ℓ_D, and height, h_D, at the onset of loading as depicted in Fig. 9(b). Within the present simplification, the delamination crack is viewed as a thin rectangular slab embedded into the specimen center plane and centered at the crack tip. Fig. 9(c) shows the highly refined finite element mesh defining the delamination crack region in which the size of the square elements within the thin slab is 0.025 mm. Guided by experimental observations made by Alam et al. [103] and following previous work by Kalyanam et al. [106], the delamination sizes (as characterized by the length, ℓ_D, and the height, h_D) adopted in the present study are taken as 0.5×0.25 mm, 1×0.5 mm and 2×1 mm. This range of sizes provides a close representation of the observed delamination crack sizes and shapes with increased load levels up to a maximum K_J-value of 100 MPa$\sqrt{\text{m}}$ which is in accord with the upper shelf fracture toughness measured in the fracture testing conducted by Alam et al. [103]. Moreover, while the adopted approach does not consider the growth of the delamination crack with increased loading, thereby not including history effects on the evolving crack front stress fields and crack front constraint, it is adequately descriptive of the local conditions affecting macroscopic fracture behavior in conventional fracture specimens with a crack-divider delamination. The numerical solutions to analyze delamination cracking effects on fracture behavior based on the Weibull stress described next utilize an elastic-plastic constitutive model with J_2 flow theory and conventional Mises

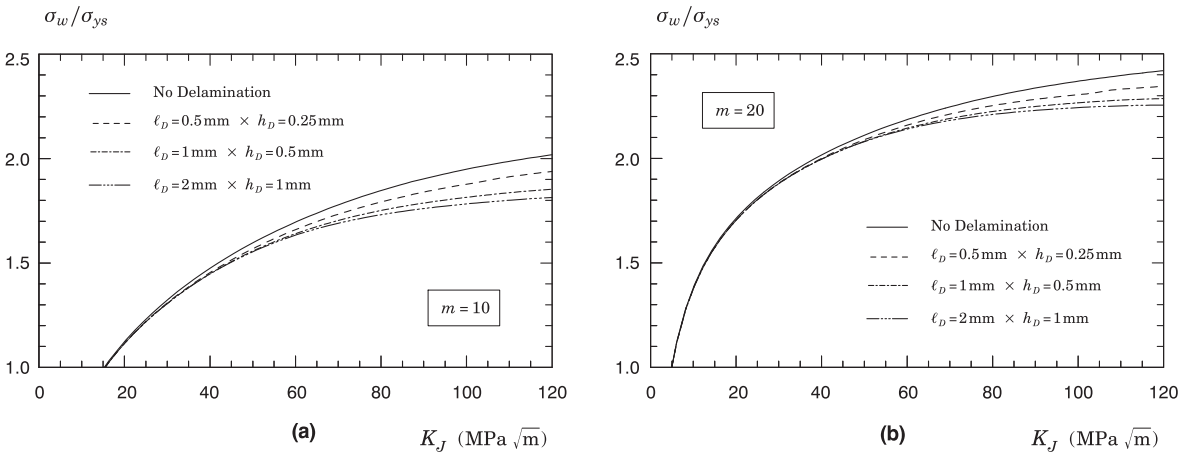

Fig. 10. Weibull stress trajectories with increased remote loading, K_J, for the plane-sided SE(B) specimen with and without transverse delamination crack made of an NFA material tested by Alam et al. [103] for varying Weibull moduli: (a) $m = 10$; (b) $m = 20$.

plasticity in large geometry change (LGC) setting incorporating a piecewise linear approximation to the measured tensile response for the tested high strength nanostructured ferritic (14YWT) alloy reported by Alam et al. [103]. The present results focus on the numerical solutions corresponding to the mechanical and flow properties at the test temperature $T = -150\,^{\circ}$C. The finite element code WARP3D [107] provides the numerical solutions for the 3-D analyses reported here.

Following the methodology outlined previously (see also Ruggieri and Dodds [6], under increased remote loading (as measured by K_J in the present context), differences in evolution of the Weibull stress reflect the potentially strong variations of near-tip stress fields due to the coupling effect of constraint loss and delamination cracking, which has a direct bearing on the macroscopic fracture behavior for the analyzed fracture specimen. Further, the variation of macroscale crack driving force (K_J) resulting from delamination cracking effects in the 3-D SE(B) models is then characterized by the toughness scaling model based upon the standard Beremin Weibull stress, σ_w, and the resulting fracture toughness ratios for the fracture specimens with and without delamination. In these analyses, the σ_w vs. K_J trajectories are determined for two different values of the Weibull modulus, $m = 10$ and 20. These values are representative of typical structural ferritic steels and well in accord with previous reported values. A value of $m = 20$ is mostly appropriate for ferritic material exhibiting moderate hardening behavior such as the nanoferritic alloy at $T = -150\,^{\circ}$C utilized in this study (see Alam et al. [103]).

Fig. 10(a) and (b) illustrate the effect of delamination crack size on the σ_w vs. K_J trajectories for the plane-sided model with $m = 10$ and 20. In these plots, the Weibull stress, σ_w, is normalized by the material yield stress at $T = -150\,^{\circ}$C. The trend is clear. In the initial stage of load level, all curves collapse onto a single trajectory indicating essentially no effect of transverse delamination on macroscopic fracture. After this transitional behavior, the value of σ_w is reduced (relative to the model with no delamination) with increased delamination size as deformation progresses. Observe that the effect of delamination on macroscopic fracture behavior is more prominent for the numerical models having a small-to-moderate delamination crack sizes (0.5×0.25 mm and 1×0.5 mm delaminations), which is entirely consistent with the evolution of crack-front stress contours already shown previously. Fig. 11(a) and (b) recast these σ_w vs. K_J trajectories for the plane-sided model into the form of toughness ratios defined by $K_J^{Nodelam} \rightarrow K_J^{Delam}$ for varying delamination sizes and different Weibull moduli, m, as derived directly from the toughness scaling model outlined in Ruggieri and Dodds [6]. Each curve provides pairs of K_J-values in the SE(B) specimens with and without delamination which produce the same Weibull stress, $\tilde{\sigma}_w$, for a fixed m-value. Further, within the present context of probabilistic fracture mechanics, each pair $(K_J^{Nodelam}, K_J^{Delam})$ on a given delamination size curve defines equal failure probabilities for cleavage fracture. A reference line is shown which defines a unit toughness ratio defined by $K_J^{Nodelam} = K_J^{Delam}$. These results clearly show the influence of a transverse delamination in increasing an effective K_J-value at fracture. Significant observations from these plots include: (1) The curves for each delamination size agree very well early in the loading history while the perturbation in the crack-front stresses (due to the transverse delamination) is relatively weak associated with small fracture process zone sizes; (2) Once the stress-free surface at the center plane (associated with the transverse delamination) relaxes the through-thickness constraint, the curves for the numerical models with delamination fail to increase at the same rate with further loading thereby clearly showing the gradual nature of constraint loss with increased loading due to transverse splitting; (3) The Weibull modulus does not have an appreciable effect on the resulting toughness ratios for the analyzed crack configurations; here, the $K_J^{Nodelam} \rightarrow K_J^{Delam}$ are only weakly sensitive to the adopted m-values and (4) Similar to the previous observations, the effect of delamination on the resulting toughness ratios is more prominent for the numerical models having a small-to-moderate delamination crack sizes (0.5×0.25 mm and 1×0.5 mm delaminations).

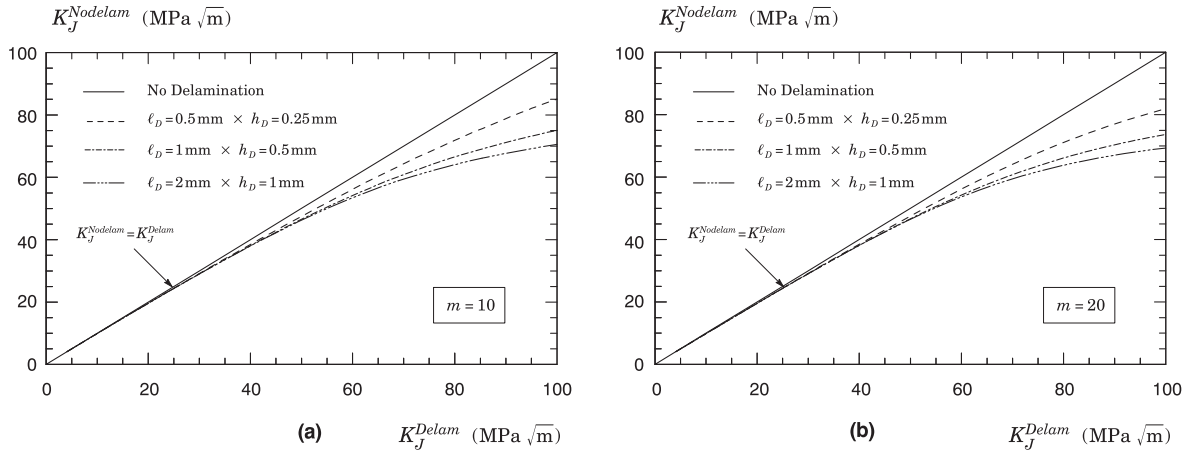

Fig. 11. Toughness ratios in terms of K_J-values for the plane-sided SE(B) specimen made of an NFA material tested by Alam et al. [103] with varying transverse delamination crack sizes and different Weibull moduli: (a) $m = 10$; (b) $m = 20$.

In using these results to discuss the effects of transverse delamination cracking on the cleavage fracture behavior, it is well to keep in mind the relatively simplified nature of these analyses. As already hinted, the adopted approach does not consider the growth of the delamination crack with increased loading and, thus, does not include history effects on the evolving crack front stress fields and crack front constraint. Further, the 3-D FE models for the SE(B) specimens, albeit highly refined, consider only one transverse, central delamination crack. Alam et al. [103] observed the formation of several delamination cracks (splits) extending over a large fraction of the remaining crack ligament as much as $\approx 0.8-1.2$ mm from the crack tip and having delamination planes normal to both the extrusion and cross rolling directions. Finally, computation of the evolution of σ_w with K_J considers only the principal stress criterion. Since the delamination cracks occur when the near-tip stresses acting along the through-thickness direction (Z) reach a critical value [101] thereby causing fracture of the weak planes (most often by a transgranular cleavage mechanism) and creating a macroscopically transverse planar crack, it should be expected that the fracture criterion entering into the Weibull stress computation should also reflect the potential changes in the out-of-plane stresses after the formation of a transverse crack (see Kalyanam et al. [106]). Nevertheless, the Weibull stress approach briefly described here shows promise as an engineering procedure for assessing the effects of delamination cracking on fracture toughness for ferritic materials.

4.8. Extension to other brittle fracture problems

Most of the applications of the Weibull stress approach discussed briefly earlier (see also R&D [6], Pineau [3], Pineau et al. [45] and references therein) have the common feature of involving homogeneous ferritic materials, typically represented by pressure vessel steels. Despite additional potential difficulties, extensions of the methodology to address some classes of problems related to brittle fracture may be expected to provide reasonable descriptions of fracture behavior based on the Weibull stress concept. While we would hesitate to generalize such a broad statement, a case of considerable interest involves the assessment of hydrogen embrittlement (HE) and hydrogen-induced cracking (HIC) in high strength steels.

HE and HIC represent a complex phenomenon of material degradation for which several mechanisms related to its kinetic process are not well understood at the fundamental level. For structural ferritic steels, however, hydrogen-induced transgranular cleavage fracture is relatively well understood and often attributed to the formation of incipient cracks by the precipitation of molecular hydrogen that meet the Griffith condition of crack instability [108]. While there is still strong debate over the hydrogen embrittlement mechanisms that control the cleavage and quasi-cleavage fracture due to hydrogen [109], the underlying features and importance of HE and HIC in many engineering applications largely justify further extensions of the Weibull stress approach to address the influence of hydrogen embrittlement in reducing fracture toughness of structural steels. However, there are, at present, only few studies adopting LAF methodologies to evaluate the effects of HE and HIC phenomena on fracture behavior of ferritic materials, including the works of Takagi et al. [110,111] and Ohata [112]. In particular, by adopting an alternative form of the Weibull stress incorporating the local stresses and the reduction in content of cohesive energy diffusible hydrogen, Ohata et al. [112] were able to assess the susceptibility of hydrogen-induced fracture for the specimens tested in their study. While these analyses and results seem consistent with the present level of development of the Weibull stress framework, they remain rather untested as a robust and verified methodology to address HE and HIC related fracture in structural steels. A similar approach based on the Weibull stress concept has also been adopted in previous work of Malaplate et al. [113] to assess the effects of He on the degradation of fracture toughness for a 9Cr-1Mo steel.

5. Concluding remarks

One objective of this brief review is to summarize recent advances in the local approach to cleavage fracture modeling, illustrated by selected examples of application to predict effects of specimen geometry on cleavage fracture toughness for typical pressure vessel steels. In particular, it has been shown the effectiveness of a modified form of the Weibull stress incorporating the influence of plastic strain on the number of eligible Griffith-like microcracks nucleated from brittle particles dispersed into the ferrite matrix on fracture assessments and toughness predictions for low constraint crack configurations. Another objective of this work is to discuss some key features associated with the robustness of the Weibull stress approach while, at the same time, considering some challenges for potential new extensions and applications. These new research initiatives cover many fracture problems involving collective microfeatures that are intrinsically complex to capture in a rather simplified model, ranging from loading rate effects, materials with macroscopic heterogeneities, delamination effects of fracture and material degradation by hydrogen embrittlement (HE) and hydrogen-induced cracking (HIC).

Specifically for the conventional cases of multiscale predictions of fracture behavior in structural components with diverse range of crack-tip constraint, inclusion of the effect of near-tip plastic strain on cleavage microcracking which impacts directly the magnitude of the Weibull stress appear central to derive improved toughness scaling corrections and, consequently, to obtain more accurate fracture toughness predictions. Adoption of a modified form of the Weibull stress incorporating plastic strain effects does appear to bring fracture toughness predictions into better agreement with experimental measurements. Nevertheless, we raise another line of argument that goes beyond the interpretation of plastic strain as a computed quantity that simply represents implicitly a rather complex coupling of different microfeatures (mostly unknown) such as microcrack blunting, microvoid formation and a more realistic Griffith fracture criterion at the microscale, among others, and essentially serves to provide better fitting of the Weibull stress parameters in the present framework. The influence of plastic strain is viewed as a key crack tip quantity (as much as the principal stresses) effectively driving the microprocess of cleavage fracture and strongly linked to fracture mechanism. Such arguments thus motivate the interpretation of the plastic strains acting inside the fracture process zone ahead of crack tip as a proxy for more complex, interacting deformations mechanisms over grain size length scales.

Powerful computational resources now available offer a route for large scale simulations of different structural components having crack-like flaws allowing a relatively rapid and detailed description of their mechanical (global) response and associated local stress-strain fields. However, to obtain meaningful predictions which are reasonably invariant to model details, including crack and loading configuration, there are still restrictions imposed by our current understanding of the methodology and its fundamental concepts. Moreover, the need to incorporate all the relevant mechanical and metallurgical microfeatures into the model to obtain a more accurate description of the physical mechanism (thereby placing emphasis on developing a more fundamental, scientific model) should be tempered by the need to develop a relatively simpler, but yet highly effective, engineering model capable of dealing with complex situations with only modest effort. The authors hope that the present article and the work described herein will encourage further developments in local approach to cleavage fracture modeling.

Acknowledgments

This investigation is supported by Fundação de Amparo à Pesquisa do Estado de São Paulo (FAPESP) through Grant 2016/26024-1 and by the Brazilian Council for Scientific and Technological Development (CNPq) through Grant 306193/2013–2.

Appendix A. Supplementary material

Supplementary data associated with this article can be found, in the online version, at https://doi.org/10.1016/j.engfracmech.2017.12.021.

References

[1] Beremin FM. A local criterion for cleavage fracture of a nuclear pressure vessel steel. Metall Mater Trans A 1983;14:2277–87.
[2] Mudry F. A local approach to cleavage fracture. Nucl Eng Des 1987;105:65–76.
[3] Pineau A. Development of the local approach to fracture over the past 25 years: theory and applications. Int J Fract 2006;138:139–66.
[4] Ruggieri C, Dodds RH. A transferability model for brittle fracture including constraint and ductile tearing effects: a probabilistic approach. Int J Fract 1996;79:309–40.
[5] Ruggieri C. Influence of threshold parameters on cleavage fracture predictions using the Weibull stress model. Int J Fract 2001;110:281–304.
[6] Ruggieri C, Dodds RH. An engineering methodology for constraint corrections of elastic-plastic fracture toughness – Part I: A review on probabilistic models and exploration of plastic strain effects. Eng Fract Mech 2015;134:368–90.
[7] Ruggieri C, Savioli RG, Dodds RH. An engineering methodology for constraint corrections of elastic-plastic fracture toughness – Part II:: Effects of specimen geometry and plastic strain on cleavage fracture predictions. Eng Fract Mech 2015;146:185–209.
[8] Hahn GT. The influence of microstructure on brittle fracture toughness. Metall Trans A 1984;15:947–59.
[9] McMahon CJ, Cohen M. Initiation of cleavage in polycrystalline iron. Acta Metall 1965;13:591–604.
[10] Kaechele LE, Tetelman AS. A statistical investigation of microcrack formation. Acta Metall 1969;17:463–75.
[11] Brindley BJ. The effect of dynamic strain-aging on the ductile fracture process in mild steel. Acta Metall 1970;18:325–9.
[12] Lindley TC, Oates G, Richards CE. A critical appraisal of carbide cracking mechanism in ferritic/carbide aggregates. Acta Metall 1970;18:1127–36.

[13] Gurland J. Observations on the fracture of cementite particles in a spheroidized 1.05% C steel deformed at room temperature. Acta Metall 1972;20:735–41.
[14] Weibull W. The phenomenon of rupture in solids, Handlingar 153, Ingeniors Vetenskaps Akademien; 1939.
[15] Weibull W. A statistical theory of the strength of materials, Handlingar 151, Ingeniors Vetenskaps Akademien; 1939.
[16] Epstein B. Statistical aspects of fracture problems. J Appl Phys 1948;19:140–7.
[17] Freudenthal AM. Statistical approach to brittle fracture. In: Liebowitz H, editor. Fracture: an advanced treatise, vol. II. New York: Academic Press; 1968. p. 592–619. Ch. 6.
[18] Fisher RA, Tippet LHC. Limiting forms of the frequency distribution of the largest and smallest member of a sample. Proc Cambr Philos Soc 1928;24:180–90.
[19] Gumbel EJ. Statistics of extremes. New York: Columbia University Press; 1958.
[20] Evans AG, Langdon TG. Structural ceramics. In: Chalmers B, editor. Progress in materials science, vol. 21. New York: Pergamon Press; 1976. p. 171–441.
[21] McClintock FA, Argon AS. Mechanical behavior of materials. Reading, Massachussets: Addison-Wesley; 1966.
[22] Batdorf SB, Crose JG. A statistical theory for the fracture of brittle structures subjected to nonuniform polyaxial stresses. J Appl Mech 1974;41:459–64.
[23] Evans AG. A general approach for the statistical analysis of multiaxial fracture. J Am Ceram Soc 1978;61:302–8.
[24] McClintock FA, Zaverl JR. An analysis of the mechanism and statistics of brittle crack initiation. Int J Fract 1979;15:107–18.
[25] Matsuo Y. Statistical theory for multiaxial stress states using Weibull's three-parameter function. Eng Fract Mech 1981;14:527–38.
[26] Lin T, Evans AG, Ritchie RO. A statistical model of brittle fracture by transgranular cleavage. J Mech Phys Solids 1986;21:263–77.
[27] Godse R, Gurland J. A statistical model for low temperature cleavage fracture in mild steels. Acta Metall 1989;37:541–8.
[28] Wallin K, Saario T, Törrönen K. Statistical model for carbide induced brittle fracture in steel. Metal Sci 1984;18:13–6.
[29] Wallin K, Laukkanen A. New developments of the Wallin, Saario, Törrönen cleavage fracture model. Eng Fract Mech 2008;75:3367–77.
[30] Pineau A. Global and local approaches of fracture – transferability of laboratory test results to components. In: Argon AS, editor. Topics in fracture and fatigue. Springer Verlag; 1992. p. 197–234.
[31] Minami F, Brückner-Foit A, Munz D, Trolldenier B. Estimation procedure for the Weibull parameters used in the local approach. Int J Fract 1992;54:197–210.
[32] Gao X, Ruggieri C, Dodds RH. Calibration of Weibull stress parameters using fracture toughness data. Int J Fract 1998;92:175–200.
[33] Petti JR, Dodds RH. Calibration of the Weibull stress scale parameter, σ_u, using the master curve. Eng Fract Mech 2005;72:91–120.
[34] Ruggieri C. An engineering methodology to assess effects of weld strength mismatch on cleavage fracture toughness using the Weibull stress approach. Int J Fract 2010;164:231–52.
[35] Margolin BZ, Shvetsova VA. Local criterion to for cleavage fracture: structural and mechanical approach. J Phys IV 1996;6:225–34.
[36] Margolin BZ, Shvetsova VA, Gulenko AG, Kostylev VI. Prometey local approach to brittle fracture: development and application. Eng Fract Mech 2008;75:3483–98.
[37] Margolin BZ, Shvetsova VA, Gulenko AG. Radiation embrittlement modeling in multi-scale approach to brittle fracture of RPV steels. Int J Fract 2012;179:87–108.
[38] Faleskog J, Kroon M, Öberg H. A probabilistic model for cleavage fracture with a length scale – parameter estimation and predictions of stationary crack experiments. Eng Fract Mech 2004;71:57–79.
[39] Kroon M, Faleskog J. A probabilistic model for cleavage fracture with a length scale influence of material parameters and constraint. Int J Fract 2002;118:99–118.
[40] Hohe J, Friedmann V, Wenck J, Siegele D. Assessment of the role of micro defect nucleation in probabilistic modeling of cleavage fracture. Eng Fract Mech 2008;75:3306–27.
[41] Hohe J, Hardenacke V, Luckow S, Siegele D. An enhanced probabilistic model for cleavage fracture assessment accounting for local constraint effects. Eng Fract Mech 2010;77:3573–91.
[42] Hohe J, Luckow S, Hardenacke V, Sguaizer Y, Siegele D. Enhanced fracture assessment under biaxial external loads using small scale cruciform bending specimens. Eng Fract Mech 2011;78:1876–94.
[43] James P, Ford M, Jivkov A. A novel particle failure criterion for cleavage fracture modelling allowing measured brittle particle distributions. Eng Fract Mech 2014;121–122:98–115.
[44] Pineau A, Tanguy B. Advances in cleavage fracture modelling in steels: micromechanical. numerical and multiscale aspects. C.R. Phys. 2010;11:316–25.
[45] Pineau A, Benzerga AA, Pardoen T. Failure of metals I: brittle and ductile fracture. Acta Mater 2016;107:424–83.
[46] Averbach BL. Micro and macro formation. Int J Fract Mech 1965;1:272–90.
[47] Tetelman AS, McEvily AJ. Fracture of structural materials. New York: John Wiley & Sons; 1967.
[48] Smith E. Cleavage fracture in mild steel. Int J Fract Mech 1968;4:131–45.
[49] Low JR. Relation of properties to microstructure. Trans Am Soc Metals 1953;46A:163–79.
[50] Owen WS, Averbach M, Cohen BL. Brittle fracture in mild steel in tension at −196 c. Trans Am Soc Metals 1958;50:634–55.
[51] Griffith AA. The phenomenon of rupture and flow in solids. Philos Trans Roy Soc, Ser A 1921;221:163–98.
[52] Feller W. Introduction to probability theory and its application, vol. I. New York: John Wiley & Sons; 1957.
[53] Mann NR, Schafer RE, Singpurwalla ND. Methods for statistical analysis of reliability and life data. New York: Jonh Wiley & Sons; 1974.
[54] Lei WS. A cumulative failure probability model for cleavage fracture in ferritic steels. Mech Mater 2016;93:184–98.
[55] Lei WS. A discussion of an engineering methodology for constraint corrections of elastic-plastic fracture toughness – Part II: Effects of specimen geometry and plastic strain on cleavage fracture predictions by C. Ruggieri, R.G. Savioli, R.H. Dodds. Eng Fract Mech 2017;178:527–34.
[56] Xia L, Shih CF. Ductile crack growth – III: transition to cleavage fracture incorporating statistics. J Mech Phys Solids 1996;44:603–39.
[57] Bordet SR, Karstensen AD, Knowles DM, Wiesner CS. A new statistical local criterion for cleavage fracture in steel. Part I: Model presentation. Eng Fract Mech 2005;72:435–52.
[58] Bordet SR, Karstensen AD, Knowles DM, Wiesner CS. A new statistical local criterion for cleavage fracture in steel. Part II: Application to an offshore structural steel. Eng Fract Mech 2005;72:453–74.
[59] James PM, Ford M, Jivkov AP. A novel particle failure criterion for cleavage fracture modelling allowing measured brittle particle distributions. Eng Fract Mech 2014;121–122:98–115.
[60] American Society for Testing and Materials, Standard specification for pressure vessel plates, carbon steel, for intermediate- and higher-temperature service, ASTM A515; 2010.
[61] Savioli RG, Ruggieri C. Experimental study on the cleavage fracture behavior of an ASTM A285 Grade C pressure vessel steel. ASME J Press Vessel Technol 2014;137(2):1–7.
[62] American Society for Testing and Materials, Standard specification for pressure vessel plates, carbon steel, low- and intermediate-tensile strength, ASTM A285; 2012.
[63] American Society for Testing and Materials, Standard test method for measurement of fracture toughness, ASTM E1820-15; 2015.
[64] American Society for Testing and Materials, Standard test method for determination of reference temperature, T_0, for ferritic steels in the transition range, ASTM E1921-16; 2016.
[65] Ruggieri C. A probabilistic model including constraint and plastic strain effects for fracture toughness predictions in a pressure vessel steel. Int J Press Vessels Pip 2016;148:9–25.

[66] Ruggieri C. WSTRESS Release3.0: numerical evaluation of probabilistic fracture parameters for 3-D cracked solids and calibration of weibull stress parameters, Tech. rep., University of S ao Paulo; 2015.
[67] Ruggieri C, Dodds RH. A Weibull stress approach incorporating the coupling effect of constraint and plastic strain in cleavage fracture toughness predictions. In: ASME 2014 pressure vessels & piping conference (PVP 2014), Anaheim, CA; 2014.
[68] Thoman DR, Bain LJ, Antle CE. Inferences on the parameters of the Weibull distribution. Technometrics 1969;11:445–60.
[69] Ruggieri C, Gao X, Dodds RH. Transferability of elastic-plastic fracture toughness using the Weibull stress approach: significance of parameter calibration. Eng Fract Mech 2000;67:101–17.
[70] Gao X, Dodds RH, Tregoning RL, Joyce JA, Link LR. A Weibull stress model to predict cleavage fracture in plates containing surface cracks. Fatigue Fract Eng Mater Struct 1999;22:481–93.
[71] Gao X, Dodds RH. Constraint effects on the ductile-to-brittle transition temperature of ferritic steels: a Weibull stress model. Int J Fract 2000;102:43–69.
[72] Gao X, Dodds RH. An engineering approach to assess constraint effects on cleavage fracture toughness. Eng Fract Mech 2001;68:263–83.
[73] Petti JR, Dodds RH. Coupling of the Weibull stress model and macroscale models to predict cleavage fracture. Eng Fract Mech 2004;71:2079–103.
[74] Ruggieri C. A modified weibull stress approach to predict specimen geometry effects on cleavage fracture toughness in a nuclear reactor pressure vessel steel, unpublished manuscript; 2015.
[75] Rathbun HJ, Odette GR, Yamamoto T, Lucas GE. Influence of statistical and constraint loss size effects on cleavage fracture toughness in the transition – a single variable experiment and database. Eng Fract Mech 2006;73:134–58.
[76] Matos CG, Dodds RH. Probabilistic modeling of weld fracture in steel frame connections – Part I: Quasi-static loading. Eng Struct 2001;23(8):1011–30.
[77] National Institute of Standards and Technology. The January 17, 1995 Hyogoken-Nambu (Kobe)earthquake, Nist special publication 901, NIST, special Publication 901; 1996.
[78] Minami F, Arimochi K. Evaluation of prestraining and dynamic loading effects on the fracture toughness of structural steels by the local approach. J Press Vessel Technol 2001;123(3):362–72.
[79] Minami F, Ohata M. Fracture mechanics assessment of beam-to-column joints subjected to cyclic and dynamic loading. Weld World 2007;51(5–6):22–33.
[80] Yamashita Y, Minami F. Constraint loss correction for assessment of CTOD fracture toughness under welding residual stress – Part I: Methodology using the equivalent CTOD ratio. Eng Fract Mech 2010;77:2213–32.
[81] Yamashita Y, Minami F. Constraint loss correction for assessment of CTOD fracture toughness under welding residual stress – Part II: Application of toughness correction methodology. Eng Fract Mech 2010;77:2419–30.
[82] Minami F, Ohata M. Constraint assessment of brittle fracture of steel components, ISO 27306 vs. FITNET FFS. Eng Fract Mech 2012;84:67–82.
[83] Minami F, Ohata M, Takashima Y, Shimanuki H, Shimada Y, Suzuki T, et al. WES 2808 for brittle fracture assessment of steel components under seismic conditions – Part I: Fracture assessment procedure. In: 21st European Conference on Fracture (ECF21), procedia structural integrity, vol. 2, Elsevier; 2016. p. 1561–8.
[84] Shimada Y, Shimanuki H, Igi S, Minami F. WES 2808 for brittle fracture assessment of steel components under seismic conditions – Part II: Change in mechanical properties of structural steels by pre-strain and dynamic loading. In: 21st European Conference on Fracture (ECF21), Procedia structural integrity, vol. 2, Elsevier; 2016. p. 1593–600.
[85] Igi S, Shimada Y, Kinefuchi M, Minami F. WES 2808 for brittle fracture assessment of steel components under seismic conditions – Part III: Change in CTOD fracture toughness of structural steels by pre-strain and dynamic loading. In: 21st European Conference on Fracture (ECF21), Procedia structural integrity, vol. 2, Elsevier; 2016. p. 1601–9.
[86] Yamaguchi T, Kinefuchi M, Igi S, Shimada Y, Takashima Y, Minami F. WES 2808 for brittle fracture assessment of steel components under seismic conditions – Part IV: Change in mechanical properties and fracture toughness of steel weld HAZ by pre-strain. In: 21st European Conference on Fracture (ECF21), Procedia structural integrity, vol. 2, Elsevier; 2016. p. 1627–34.
[87] Ohata M, Takashima Y, Minami F. WES 2808 for brittle fracture assessment of steel components under seismic conditions – Part V: Equivalent CTOD ratio for correction of constraint loss in beam-to-column connections. In: 21st European Conference on Fracture (ECF21), Procedia structural integrity, vol. 2, Elsevier; 2016. p. 1635–42.
[88] Takashima M, Ohata Y, Ishii T, Hagihara Y, Minami F. WES 2808 for brittle fracture assessment of steel components under seismic conditions – Part VI: Application of WES 2808 to beam-to-column connections. In: 21st European Conference on Fracture (ECF21), Procedia structural integrity, vol. 2, Elsevier; 2016. p. 1585–92.
[89] Gao X, Petti JP, Dodds RH. Recent developments in the Weibull stress model for prediction of cleavage fracture in ferritic steels. In: Besson J, Moinerau D, Steglich D, editors, 9th European mechanics of materials conference, École des Mines de Paris; 2006. p. 93–8.
[90] Gao X, Dodds RH. Loading rate effects on parameters of the Weibull stress model for ferritic steels. Eng Fract Mech 2005;72:2416–25.
[91] Satoh K, Toyoda M, MInami F. Effects of fracture controlling factors on cleavage fracture initiation in specimens with heterogeneity along crack front. J Jpn Weld Soc 1981;50:743–9.
[92] McGrath JT, Braid JEM. Fracture of weldments. In: Tyson WR, Mukherjee B, editors, Proceedings of the international symposium on fracture mechanics. Metallurgical Society of the Canadian Institute of Mining and Metallurgy; 1987. p. 65–79.
[93] Daniels HE. The statistical theory of the strength of bundles of threads. I. Proc Roy Soc London Ser A (Math Phys Sci) 1945;183(995):405–35.
[94] Gücer DE, Gurland J. Comparison of the statistics of two fracture modes. J Mech Phys Solids 1962;10:365–73.
[95] Harlow DG, Phoenix SL. Probability distributions for the strength of composite materials I: two-level bounds. Int J Fract 1981;17(4):347–72.
[96] Harlow DG, Phoenix SL. Probability distributions for the strength of composite materials II: a convergent sequence of tight bounds. Int J Fract 1981;17(6):601–30.
[97] Smith RL, Phoenix SL. Asymptotic distributions for the failure of fibrous materials under series-parallel structure and equal load-sharing. J Appl Mech 1981;48:75–82.
[98] McCartney LN, Smith RL. Statistical theory of the strength of bundles. J Appl Mech 1983;50:601–8.
[99] Embury DJ, Petch JN, Wraith EA, Wrigth SE. The fracture of mild steel laminates. Trans Metall Soc AIME 1967;239:114–8.
[100] Morrison WB. Influence of testing direction on the mechanical properties of wrought steel. Metals Technol 1975;2:33–41.
[101] Baldi G, Buzzichelli G. Critical stress for delamination fracture in HSLA steels. Metal Sci 1978:459–72.
[102] Rao KTV, Yu W, Ritchie RO. Cryogenic toughness of commercial aluminum-lithium alloys: role of delamination toughness. Metall Trans A 1989;20A:485–97.
[103] Alam ME, Cunningham NJ, Gragg D, Fields K, Odette GR, Hoelzer V, et al., Mechanical properties characterization of a larger best practice heat of 14YWT NFA1, Tech. Rep. DOE/ER-0313/56, Department of Energy (DOE); 2014.
[104] Hoelzer DT, Bentley J, Sokolov MA, Miller MK, Odette GR, Alinger MJ. Influence of particle dispersions on the high-temperature strength of ferritic alloys. J Nucl Mater 2007;367–370:166–72.
[105] Ruggieri C, Alam ME, Yamamoto T, Odette GR. 3-D constraint effects in subsize SE(B) specimens of NFA-14YWT with transverse delamination, unpublished manuscript; 2015.
[106] Kalyanam S, Beaudoin AJ, Dodds RH, Barlat F. Delamination cracking in advanced aluminum-lithium alloys – experimental and computational studies. Eng Fract Mech 2009;76:2174–91.
[107] Healy B, Gullerud A, Koppenhoefer K, Roy A, RoyChowdhury S, Petti J, et al. WARP3D: 3-D nonlinear finite element analysis of solids for fracture and fatigue processes, Tech. rep., University of Illinois at Urbana-Champaign; 2014, <http://code.google.com/p/warp3d>.
[108] Nagumo M. Fundamentals of hydrogen embrittlement. 1st ed. Springer; 2016.

[109] Dadfarnia M, Nagao A, Wang S, Martin ML, Somerday BP, Sofronis P. Recent advances on hydrogen embrittlement of structural materials. Int J Fract 2015;196:223–43.
[110] Takagi S, Inoue T, Tsuzaki K, Minami F. Evaluation of hydrogen embrittlement susceptibility of high strength steel. J Jpn Inst Metals 2001;65 (12):1073–81 [in Japanese].
[111] Takagi S, Terasaki S, Tsuzaki K, Inoue T, Minami F. Application of local approach to hydrogen embrittlement fracture evaluation of high strength steels. Mater Sci Forum 2007;539–543:2155–61.
[112] Ohata M, Omura T, Minami F. Weibull model for hydrogen-induced fracture of high strength steel. ISIJ Int 2012;52(2):323–8.
[113] Malaplate J, Vincent L, Averty X, Henry J, Marini B. Characterization of He embrittlement of a 9Cr-1Mo steel using local approach of brittle fracture. In: Besson J, Moinerau D, Steglich D, Editors, 9th European mechanics of materials conference. École des Mines de Paris; 2006. p. 33–8.